

**Enantioselective Synthesis of 2-Substituted-Tetrahydroisoquinolin-1-yl Glycine Derivatives  
via Oxidative Cross-Dehydrogenative Coupling of Tertiary Amines and Chiral Nickel(II)  
Glycinate**

*Shengbin Zhou, Jiang Wang, Daizong Lin, Fei Zhao, and Hong Liu\**

CAS Key Laboratory of Receptor Research

Shanghai Institute of Materia Medica, Chinese Academy of Sciences

555 Zuchongzhi Road, Shanghai 201203 (P. R. China)

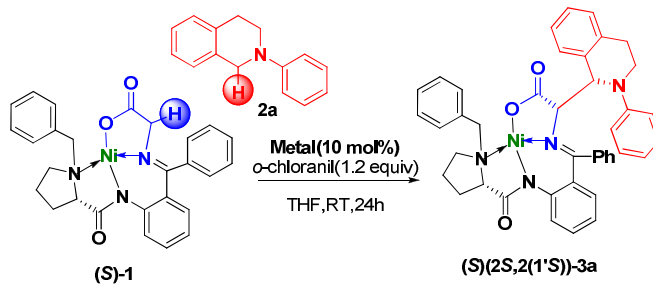
E-mail: [hliu@mail.shcnc.ac.cn](mailto:hliu@mail.shcnc.ac.cn)

**Table of Contents**

(A) Metal screening, equivalent, and temperature optimization.....	S2
(B) Mechanistic experiments and proposed reaction pathways.....	S4
(C) Stereochemical Transition of CDC.....	S5
(D) The Absolute Configuration of 3a- <i>syn</i> and 3k- <i>anti</i> .....	S6
(E) HPLC spectra for <i>de</i> determination .....	S8
(F) Copies of $^1\text{H}$ NMR and $^{13}\text{C}$ NMR Spectra for the Products.....	S17
(G) References.....	S37

**(A) Metal screening, equivalent, and temperature optimization**

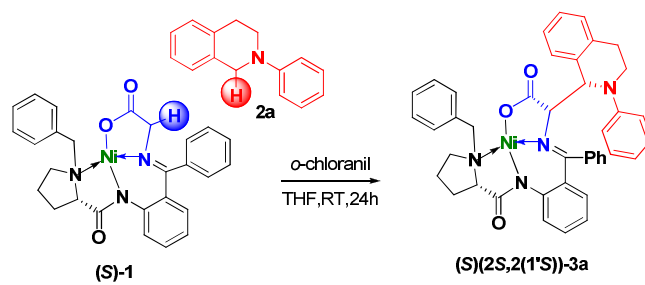
**Table S1:** Metal screening for the *o*-chloranil mediated CDC reaction.<sup>a</sup>



Entry	Metal	<i>t</i> [h]	Yield [%] <sup>b</sup>	<i>syn/anti</i> <sup>c</sup>
1	CuBr	24	17	1.3:1
2	CuI	24	13	1.2:1
3	Cu(OTf)	24	15	1.1:1
4	CuBr <sub>2</sub>	24	20	1:1.2
5	Cu(OAc) <sub>2</sub>	24	25	1:2

<sup>a</sup> Reaction conditions: (S)-1 (0.1 mmol), 2a (0.12 mmol), *o*-chloranil (0.12 mmol), metal (0.01 mmol) and THF (1.0 mL). <sup>b</sup> Isolated yield of combined 3a (*syn* and *anti*). <sup>c</sup> The diastereomeric ratios of 3a determined by <sup>1</sup>H NMR.

**Table S2:** Equivalent screening for the *o*-chloranil mediated CDC reaction.<sup>a</sup>

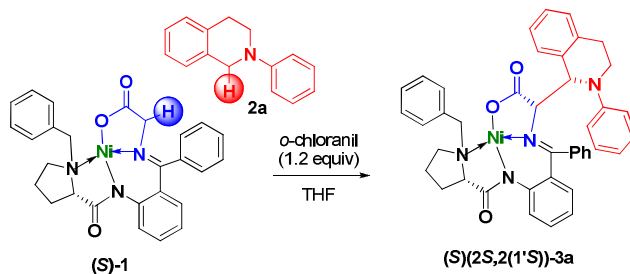


Entry	1/2a/ <i>o</i> -chloranil	<i>t</i> [h]	Yield [%] <sup>b</sup>	<i>syn/anti</i> <sup>c</sup>

1	1/1.2/1.2	24	64	4.6:1
2	1/1.2/1.5	24	50	3:1
3	1/1.5/1.2	24	65	2.5:1
4	1.2/1/1	24	55	2.8:1

<sup>a</sup> Reaction conditions: (*S*)-**1** (0.1 mmol), **2a** (0.12 mmol), *o*-chloranil (0.12 mmol), and THF(1.0 mL). <sup>b</sup> Isolated yield of combined **3a** (*syn* and *anti*). <sup>c</sup> The diastereomeric ratios of **3a** determined by <sup>1</sup>H NMR.

**Table S3:** Temperature screening for the *o*-chloranil mediated CDC reaction.<sup>a</sup>

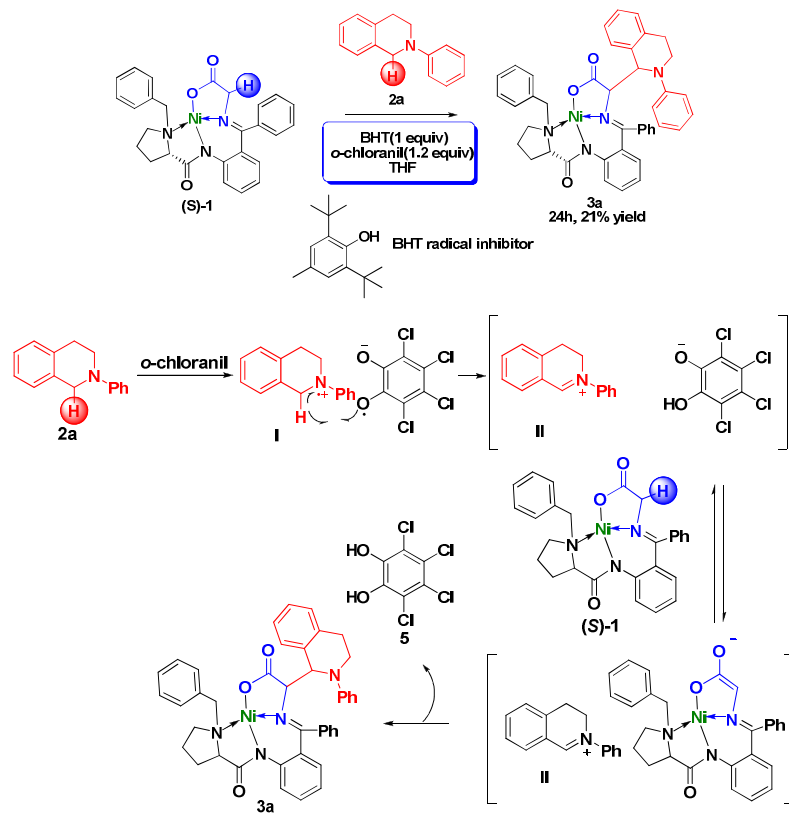


Entry	T (°C)	t [h]	Yield [%] <sup>b</sup>	<i>syn/anti</i> <sup>c</sup>
1	60	8	70	2.3:1
2	40	16	65	2.5:1
3	20	24	64	4.6:1
4	0	36	<10	n.d.
5	-20	36	0	n.d.

<sup>a</sup> Reaction conditions: (*S*)-**1** (0.1 mmol), **2a** (0.12 mmol), *o*-chloranil (0.12 mmol), and THF (1.0 mL). <sup>b</sup> Isolated yield of combined **3a** (*syn* and *anti*). <sup>c</sup> The diastereomeric ratios of **3a** determined by <sup>1</sup>H NMR. n.d. = not determined.

**(B) Mechanistic experiments and proposed reaction pathways**

The plausible reaction pathway for the coupling is postulated to involve a single-electron transfer (SET) radical mechanism<sup>1</sup> in Scheme S1. A single electron transfer from the tertiary amine **2a** to *o*-chloranil generates a radical cation **I** and a *o*-chloranil radical anion. The radical oxygen of the *o*-chloranil radical anion then abstracts  $\alpha$ -H-atom from the radical cation **I** generates the key intermediate iminium cation **II**. With one equivalent of 2,6-di-*tert*-butyl-4-methylphenol (BHT), a radical inhibitor, the yield of the coupling product decreased dramatically from 64% to 21%. These results were interpreted as the generation of radicals as key intermediate, and are in consistence with the observations by Wang *et al*<sup>2</sup> and Chi *et al*<sup>3</sup>. Then the anionic oxygen of *o*-chloranil radical anion then abstracts an  $\alpha$ -hydrogen from the glycinate to generate an enolate. Finally, the nucleophilic attack of the enolate on the iminium cation **II** generates the CDC product **3a** and the 3,4,5,6-tetrachlorobenzene-1,2-diol **5**.



**Scheme S1.** Mechanistic experiments and proposed reaction pathways

### (C) Stereochemical Transition of CDC

Considering the stereochemical outcome of the reaction under study, we could propose two transition (TS) **A** and **B** (Figure S1), leading to diastereomers *(S)(2S,2(1'S))-3/(S)(2S,2(1'R))-3* (**3-syn/3-anti**), respectively. In TS **A**, the *N*-phenyl group occupies a position of the larger substituent, thus avoiding unfavorable non-bonding interactions with the phenyl ring at the imine bond of the Ni(II) complex, which render **A** more favorable than **B**. Under optimized oxidative conditions, iminiums were attacked highly selectively from the *si*-face of Ni(II) glycinate<sup>4,5,6</sup> generating excellent diastereoselectivity. Therefore, the CDC reaction didn't generate the diastereomers *(S)(2R,2(1'R))-3/(S)(2R,2(1'S))-3*. The relative and absolute configuration of major coupling compound **3a-syn** was determined to be *(S)(2S,2(1'S))* and the minor one **3k-anti** was determined to be *(S)(2S,2(1'R))* by X-ray crystallography (Figure S3).

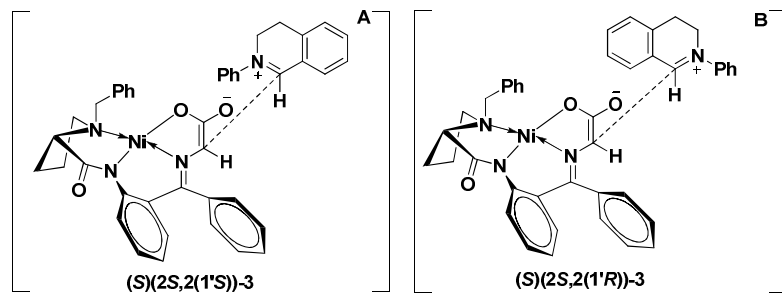


**Figure S1.** Stereochemical Transition of CDC

**(D) The Absolute Configuration of 3a-syn and 3k-anti**

X-ray Single Crystal Structure Analysis of (*S*)(2*S*,2(1'S))-**3a**:

X-ray crystallographic data of (*S*)(2*S*,2(1'S))-**3a** were solutions at T = 293(2) K; C<sub>42</sub>H<sub>38</sub>N<sub>4</sub>NiO<sub>3</sub>, M<sub>r</sub> = 705.47, monoclinic. Space group *P*2 (1), a = 15.670 (3) Å, b = 10.967 (3) Å, c = 21.785 (6) Å, α = 90°, β = 107.289 (8)°, γ = 90°, V = 3574.7 (16) Å<sup>3</sup>, Z = 4.

(*S*)(2*S*,2(1'S))-**3a**:

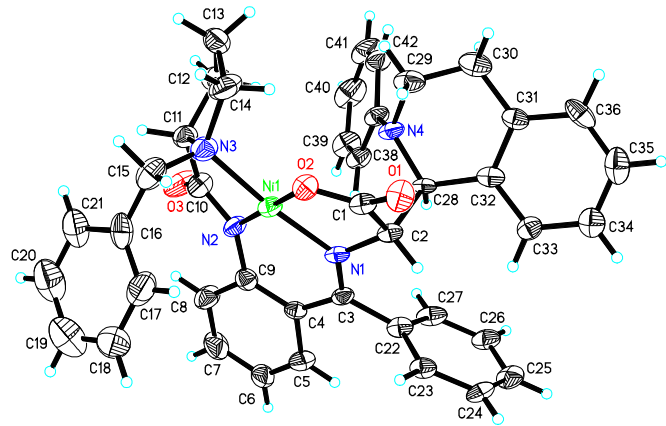


**Figure S2.** The crystal structure of (*S*)(2*S*,2(1'S))-**3a** by X-ray analysis.

(*S*)(2*S*,2(1'R))-**3k**:

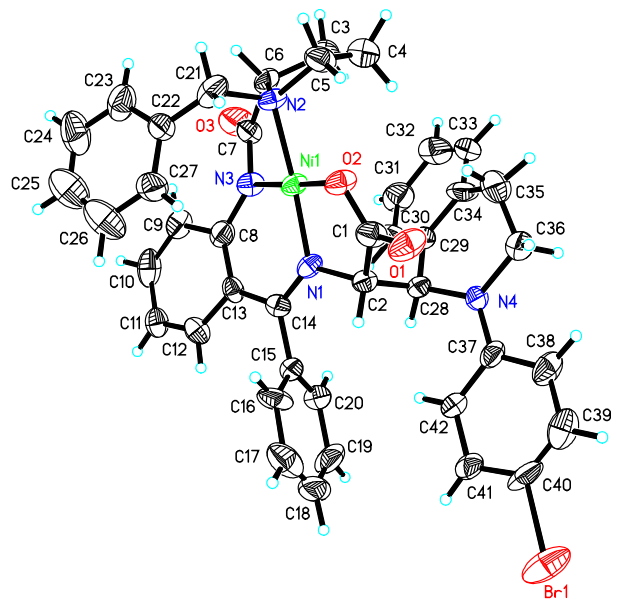
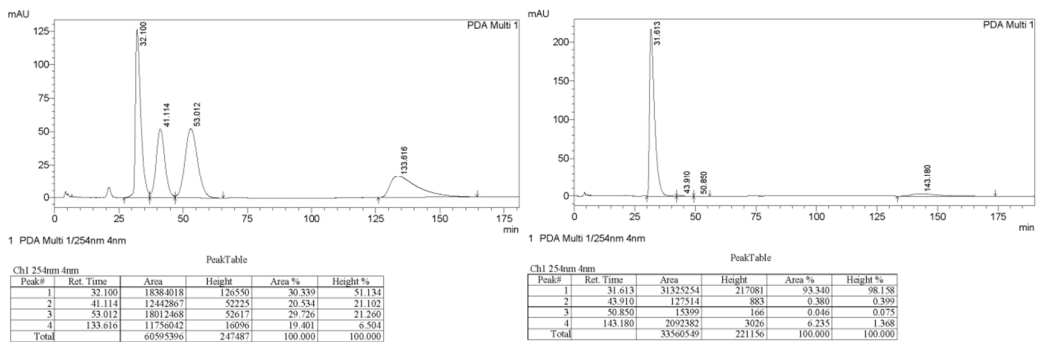


**Figure S3.** The crystal structure of  $(S)(2S,2(1'R))-3\mathbf{k}$  by X-ray analysis.

These data can be obtained free of charge from the Cambridge Crystallographic Data Centre *via* [www.ccdc.cam.ac.uk/data\\_request/cif](http://www.ccdc.cam.ac.uk/data_request/cif), the CCDC numbers are 927172 for  $(S)(2S,2(1'S))-3\mathbf{a}$ , and 962699 for  $(S)(2S,2(1'R))-3\mathbf{k}$ .

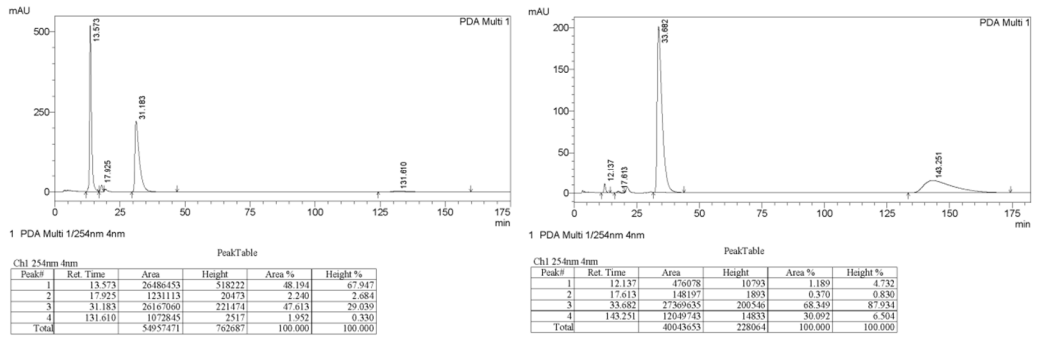
**(E) HPLC spectra for *de* determination**

**3a**



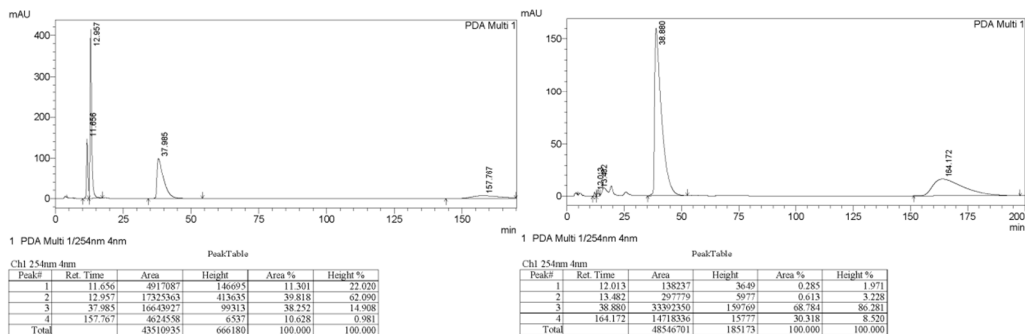
The *de* was determined by HPLC with a Chiralpak AD-H column (*n*-hexane/*i*-PrOH = 75/25,  $\lambda$  = 254 nm, 0.8 mL/min). For the *syn*-isomer:  $t_R$  (major enantiomer) = 31.61 min,  $t_R$  (minor enantiomer) = 50.85 min, > 99% *de*; for the *anti*-isomer:  $t_R$  (major enantiomer) = 143.18 min,  $t_R$  (minor enantiomer) = 43.91 min, 88% *de*.

**3b**



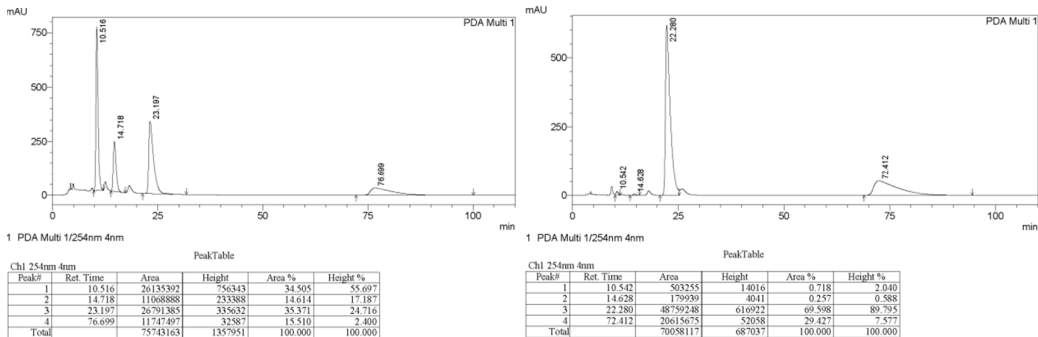
The *de* was determined by HPLC with a Chiralpak IA column (*n*-hexane/*i*-PrOH = 60/40,  $\lambda$  = 254 nm, 1.0 mL/min). For the *syn*-isomer:  $t_R$  (major enantiomer) = 33.68 min,  $t_R$  (minor enantiomer) = 12.14 min, 96% *de*; for the *anti*-isomer:  $t_R$  (major enantiomer) = 143.25 min,  $t_R$  (minor enantiomer) = 17.61 min, 97% *de*.

**3c**



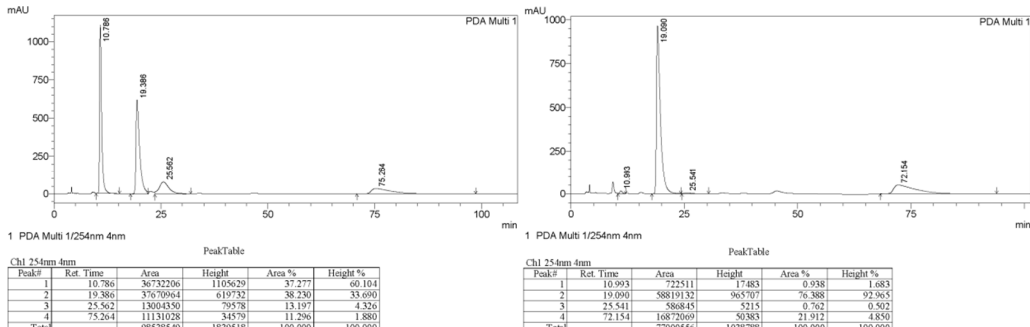
The *de* was determined by HPLC with a Chiralpak IA column (*n*-hexane/*i*-PrOH = 60/40,  $\lambda$  = 254 nm, 1.0 mL/min). For the *syn*-isomer:  $t_R$  (major enantiomer) = 38.88 min,  $t_R$  (minor enantiomer) = 13.48 min, 98% *de*; for the *anti*-isomer:  $t_R$  (major enantiomer) = 164.17 min,  $t_R$  (minor enantiomer) = 12.01 min, 98% *de*.

### 3f



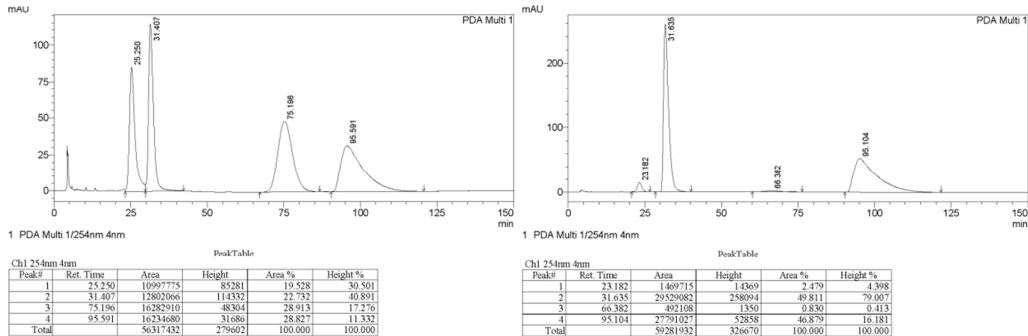
The *de* was determined by HPLC with a Chiralpak IA column (*n*-hexane/*i*-PrOH = 60/40,  $\lambda$  = 254 nm, 1.0 mL/min). For the *syn*-isomer:  $t_R$  (major enantiomer) = 22.28 min,  $t_R$  (minor enantiomer) = 10.54 min, 98% *de*; for the *anti*-isomer:  $t_R$  (major enantiomer) = 72.41 min,  $t_R$  (minor enantiomer) = 14.63 min, 98% *de*.

### 3g



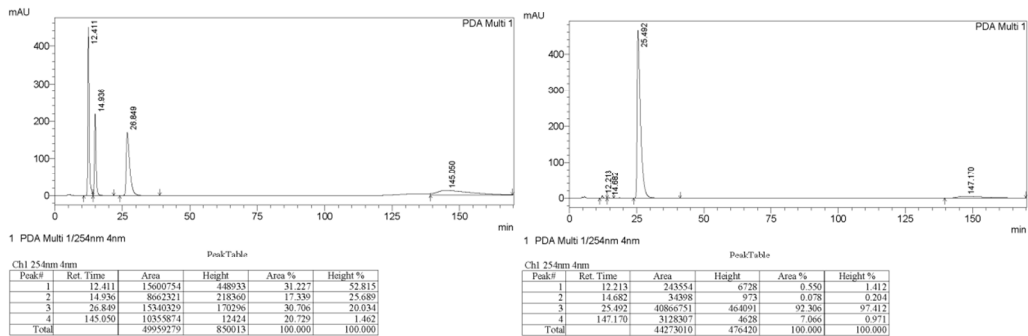
The *de* was determined by HPLC with a Chiraldak IA column (*n*-hexane/*i*-PrOH = 75/25,  $\lambda$  = 254 nm, 1.0 mL/min). For the *syn*-isomer:  $t_R$  (major enantiomer) = 19.09 min,  $t_R$  (minor enantiomer) = 10.99 min, 97% *de*; for the *anti*-isomer:  $t_R$  (major enantiomer) = 72.15 min,  $t_R$  (minor enantiomer) = 25.54 min, 98% *de*.

### 3h



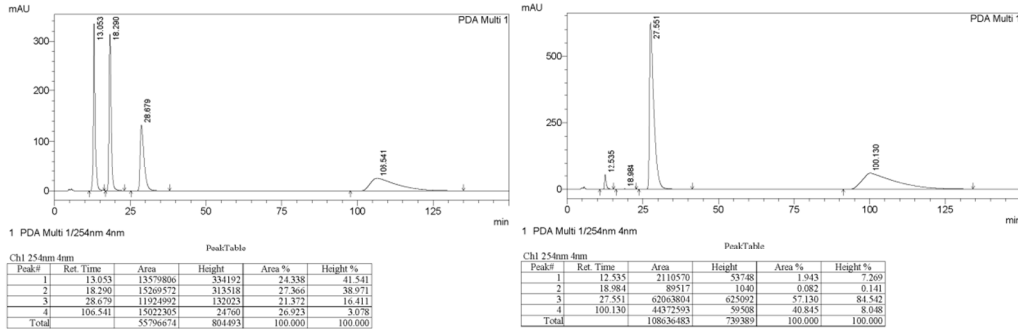
The *de* was determined by HPLC with a Chiraldak AD-H column (*n*-hexane/*i*-PrOH = 80/20,  $\lambda$  = 254 nm, 0.8 mL/min). For the *syn*-isomer:  $t_R$  (major enantiomer) = 31.64 min,  $t_R$  (minor enantiomer) = 23.18 min, 90% *de*; for the *anti*-isomer:  $t_R$  (major enantiomer) = 95.10 min,  $t_R$  (minor enantiomer) = 66.38 min, 96% *de*.

### 3i



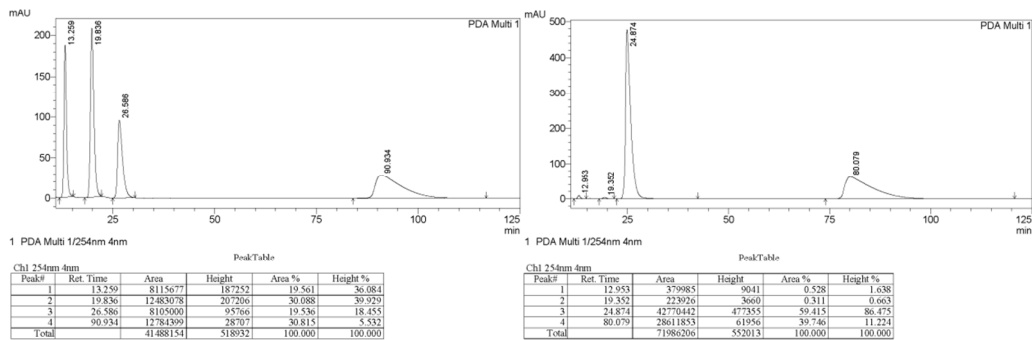
The *de* was determined by HPLC with a Chiraldak IA column (*n*-hexane/*i*-PrOH = 60/40,  $\lambda$  = 254 nm, 1.0 mL/min). For the *syn*-isomer:  $t_R$  (major enantiomer) = 25.49 min,  $t_R$  (minor enantiomer) = 12.21 min, 99% *de*; for the *anti*-isomer:  $t_R$  (major enantiomer) = 147.17 min,  $t_R$  (minor enantiomer) = 14.68 min, > 98% *de*.

### 3j



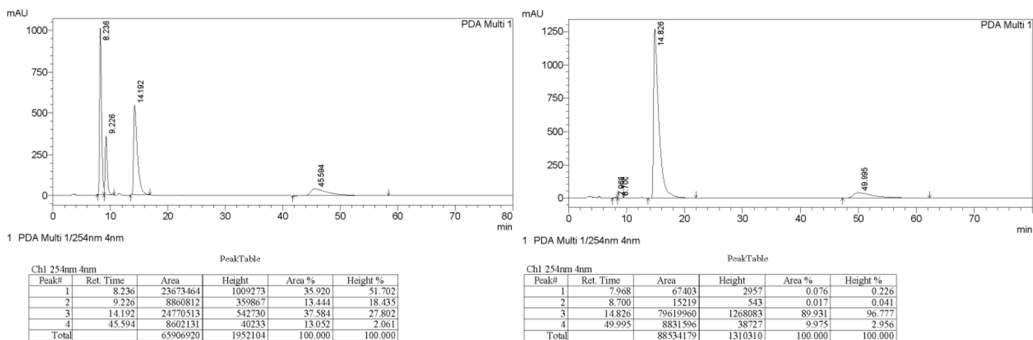
The *de* was determined by HPLC with a Chiralpak IA column (*n*-hexane/*i*-PrOH = 60/40,  $\lambda$  = 254 nm, 1.0 mL/min). For the *syn*-isomer:  $t_R$  (major enantiomer) = 27.55 min,  $t_R$  (minor enantiomer) = 12.54 min, 93% *de*; for the *anti*-isomer:  $t_R$  (major enantiomer) = 100.13 min,  $t_R$  (minor enantiomer) = 18.98 min, > 99% *de*.

### 3k



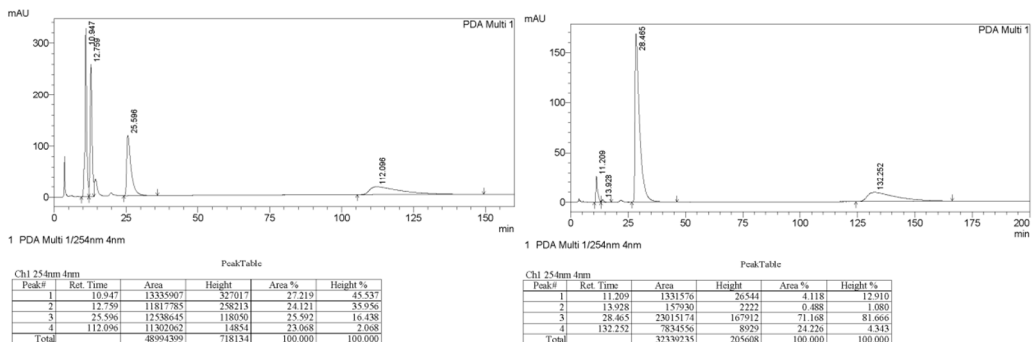
The *de* was determined by HPLC with a Chiralpak IA column (*n*-hexane/*i*-PrOH = 60/40,  $\lambda$  = 254 nm, 1.0 mL/min). For the *syn*-isomer:  $t_R$  (major enantiomer) = 24.87 min,  $t_R$  (minor enantiomer) = 12.95 min, 98% *de*; for the *anti*-isomer:  $t_R$  (major enantiomer) = 80.08 min,  $t_R$  (minor enantiomer) = 19.35 min, 98% *de*.

### 3l



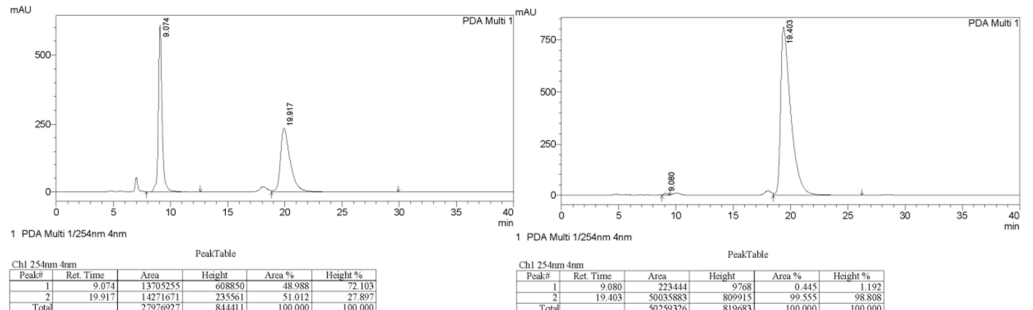
The *de* was determined by HPLC with a Chiralpak IA column (*n*-hexane/*i*-PrOH = 60/40,  $\lambda = 254$  nm, 1.0 mL/min). For the *syn*-isomer:  $t_R$  (major enantiomer) = 14.83 min,  $t_R$  (minor enantiomer) = 7.97 min, > 99% *de*; for the *anti*-isomer:  $t_R$  (major enantiomer) = 49.99 min,  $t_R$  (minor enantiomer) = 8.70 min, > 99% *de*.

### 3m



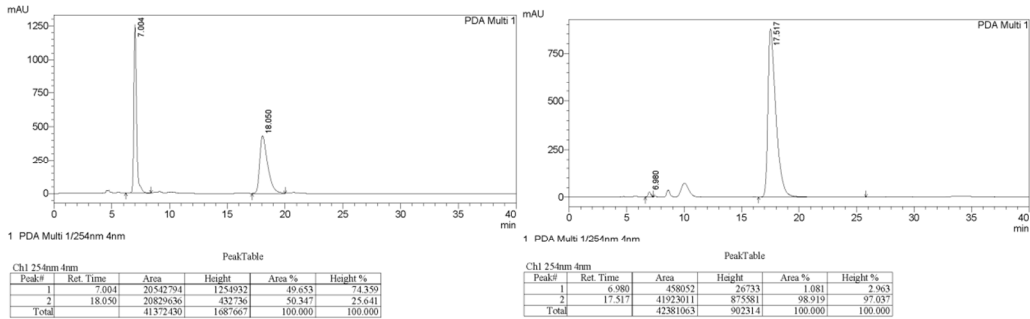
The *de* was determined by HPLC with a Chiralpak IA column (*n*-hexane/*i*-PrOH = 60/40,  $\lambda = 254$  nm, 1.0 mL/min). For the *syn*-isomer:  $t_R$  (major enantiomer) = 28.47 min,  $t_R$  (minor enantiomer) = 11.21 min, 89% *de*; for the *anti*-isomer:  $t_R$  (major enantiomer) = 132.25 min,  $t_R$  (minor enantiomer) = 13.93 min, 96% *de*.

### 3n-Syn



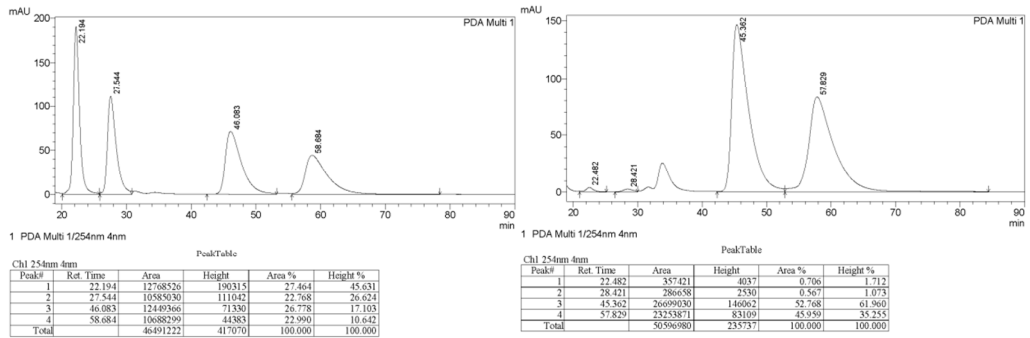
The *de* was determined by HPLC with a Chiraldak IA column (*n*-hexane/*i*-PrOH = 60/40,  $\lambda$  = 254 nm, 1.0 mL/min). For the *syn*-isomer:  $t_R$  (major enantiomer) = 19.40 min,  $t_R$  (minor enantiomer) = 9.08 min, 99% *de*.

### 3n-*anti*



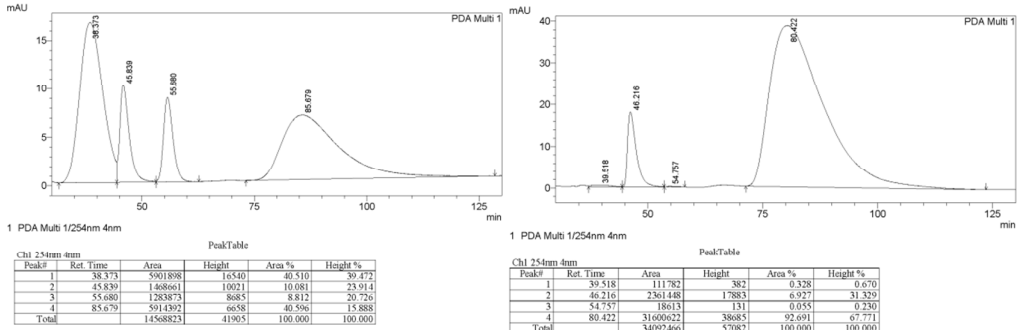
The *de* was determined by HPLC with a Chiraldak IA column (*n*-hexane/*i*-PrOH = 60/40,  $\lambda$  = 254 nm, 1.0 mL/min). For the *anti*-isomer:  $t_R$  (major enantiomer) = 17.52 min,  $t_R$  (minor enantiomer) = 6.98 min, 98% *de*.

### 3o



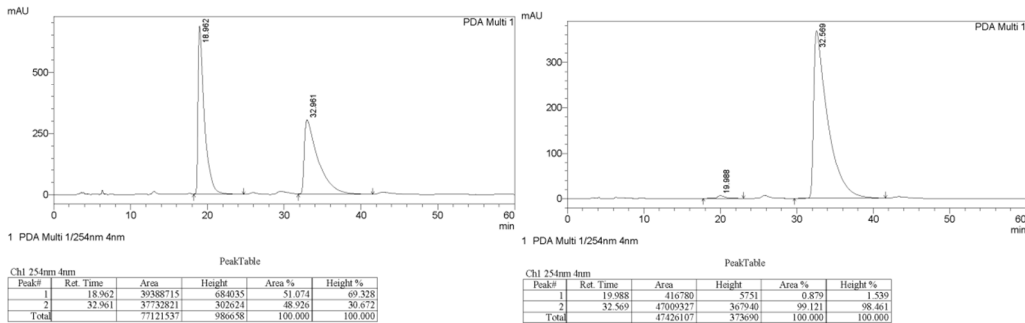
The *de* was determined by HPLC with a Chiraldak IA column (*n*-hexane/*i*-PrOH = 60/40,  $\lambda$  = 254 nm, 1.0 mL/min). For the *syn*-isomer:  $t_R$  (major enantiomer) = 45.36 min,  $t_R$  (minor enantiomer) = 22.48 min, 97% *de*; for the *anti*-isomer:  $t_R$  (major enantiomer) = 57.83 min,  $t_R$  (minor enantiomer) = 28.42 min, 97% *de*.

### 3p



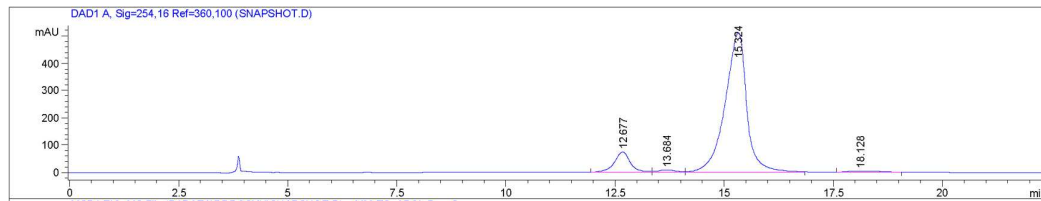
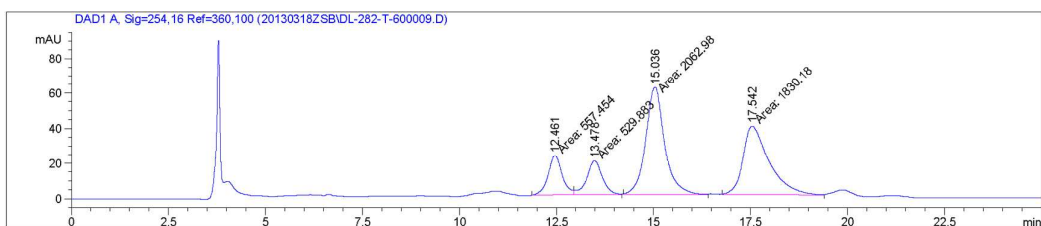
The *de* was determined by HPLC with a Chiraldak AD-H column (*n*-hexane/*i*-PrOH = 75/25,  $\lambda$  = 254 nm, 1.0 mL/min). For the *syn*-isomer:  $t_R$  (major enantiomer) = 80.42 min,  $t_R$  (minor enantiomer) = 39.52 min, 99% *de*; for the *anti*-isomer:  $t_R$  (major enantiomer) = 46.22 min,  $t_R$  (minor enantiomer) = 54.76 min, 98% *de*.

### 3q



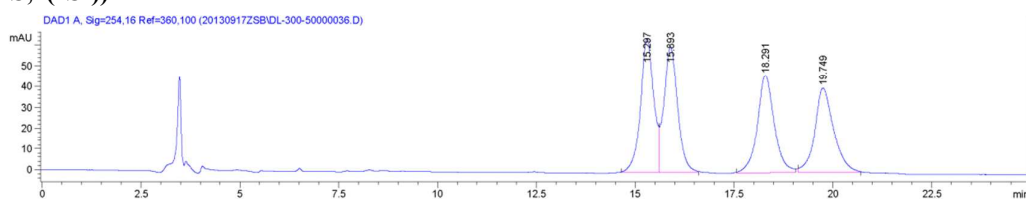
The *de* was determined by HPLC with a Chiraldak IA column (*n*-hexane/*i*-PrOH = 80/20,  $\lambda$  = 254 nm, 1.0 mL/min). For the *anti*-isomer:  $t_R$  (major enantiomer) = 32.57 min,  $t_R$  (minor enantiomer) = 19.99 min, 98% *de*.

**(2S,2(1S'))-4a**

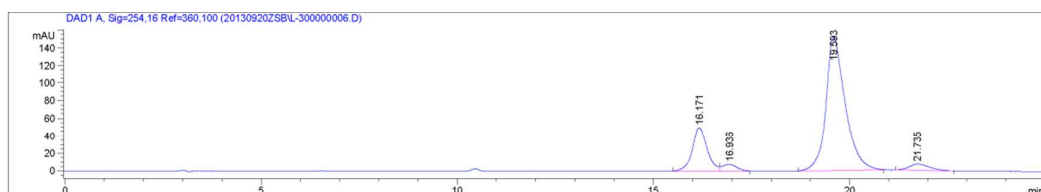


The enantiomeric excess was determined by HPLC with a Chirobiotic T column (25 cm × 4.6 mm, 5 µm) (H<sub>2</sub>O/MeOH = 60/40, λ = 254 nm, 0.5 mL/min). For the *syn*-isomer: t<sub>R</sub> (major enantiomer) = 15.32 min, t<sub>R</sub> (minor enantiomer) = 18.13 min, 98% ee; for the anti-isomer: t<sub>R</sub> (major enantiomer) = 12.68 min, t<sub>R</sub> (minor enantiomer) = 13.68 min, 80% ee.

**(2S,2(1S'))-4i**



Peak #	RetTime [min]	Type	Width [min]	Area [mAU*s]	Height [mAU]	Area %
1	15.297	BV	0.3447	1505.48865	64.41623	26.3383
2	15.893	VB	0.3588	1455.15503	60.46096	25.4577
3	18.291	BB	0.4429	1396.65552	46.70523	24.4343
4	19.749	BB	0.4914	1358.67346	40.49881	23.7698
Totals :				5715.97266	212.08124	



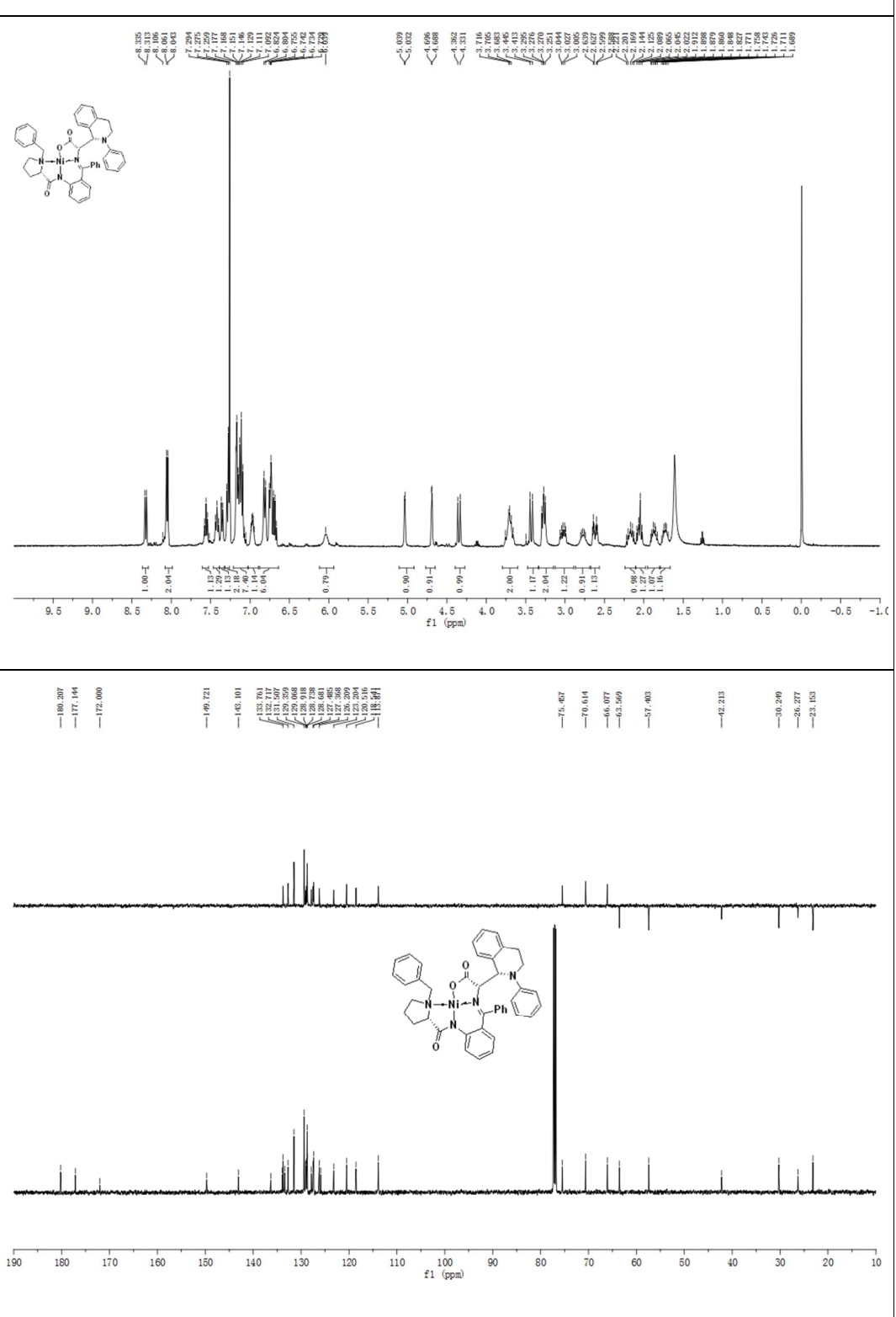
Peak #	RetTime [min]	Type	Width [min]	Area [mAU*s]	Height [mAU]	Area %
1	16.171	BV	0.3871	1303.66101	49.85438	18.6289
2	16.936	VB	0.3822	203.83260	7.81762	2.9127
3	19.593	BB	0.5022	5231.63574	152.51328	74.7585
4	21.735	BB	0.4958	258.91888	6.99586	3.6999
Totals :				6998.04823	217.18114	

The enantiomeric excess was determined by HPLC with a Chirobiotic T column (25 cm × 4.6 mm, 5 µm) ( $\text{H}_2\text{O}/\text{MeOH} = 50/50$ ,  $\lambda = 254 \text{ nm}$ , 0.5 mL/min). For the *syn*-isomer:  $t_R$  (major enantiomer) = 19.59 min,  $t_R$  (minor enantiomer) = 21.73 min, 90% ee; for the anti-isomer:  $t_R$  (major enantiomer) = 16.17 min,  $t_R$  (minor enantiomer) = 16.94 min, 73% ee.

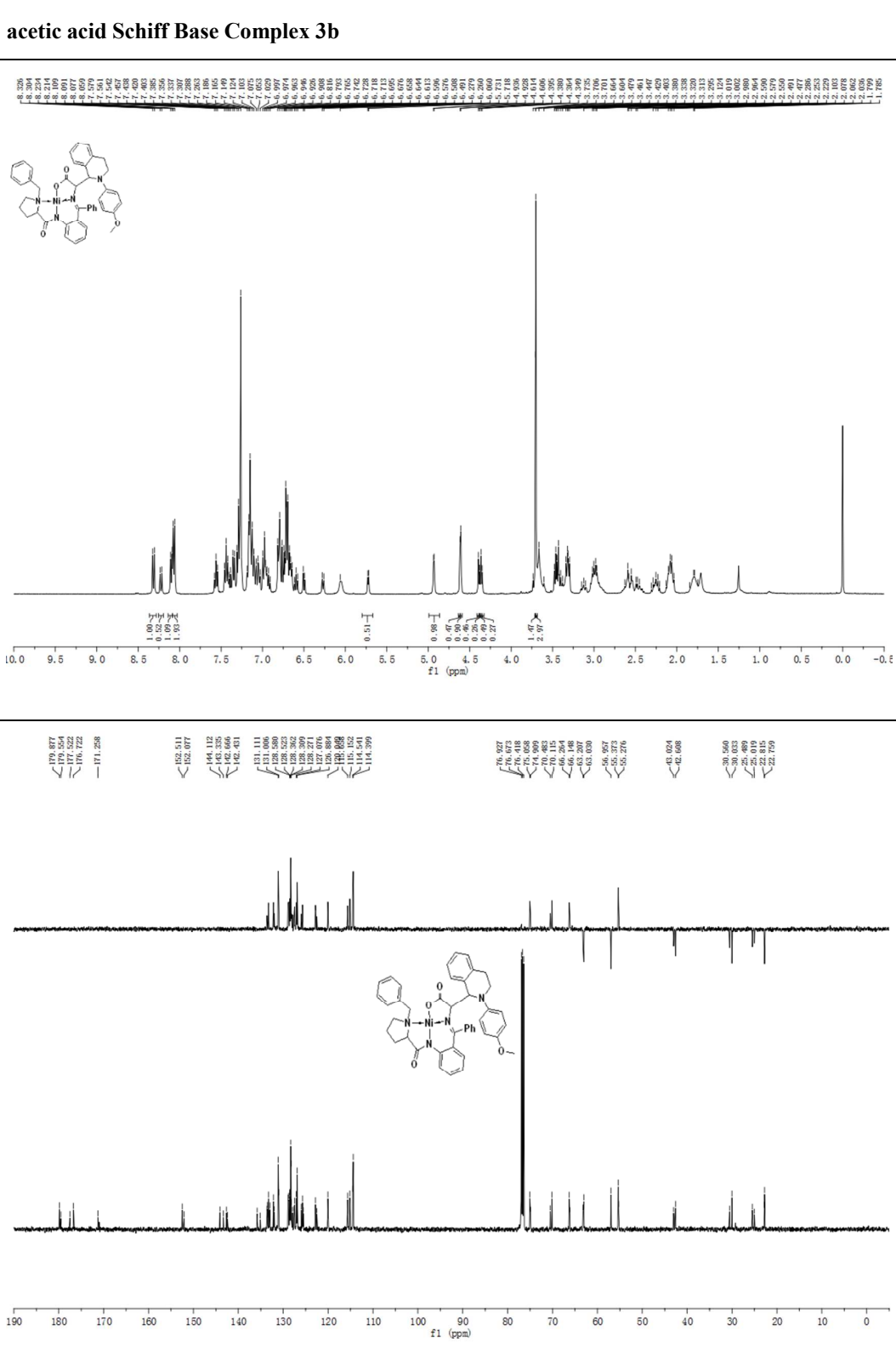
**(F) Copies of  $^1\text{H}$  NMR and  $^{13}\text{C}$  NMR Spectra for the Products**

Nickel(II)-(S)-BPB/2-Amino-2-(2-phenyl-1,2,3,4-tetrahydroisoquinolin-1-yl) acetic acid

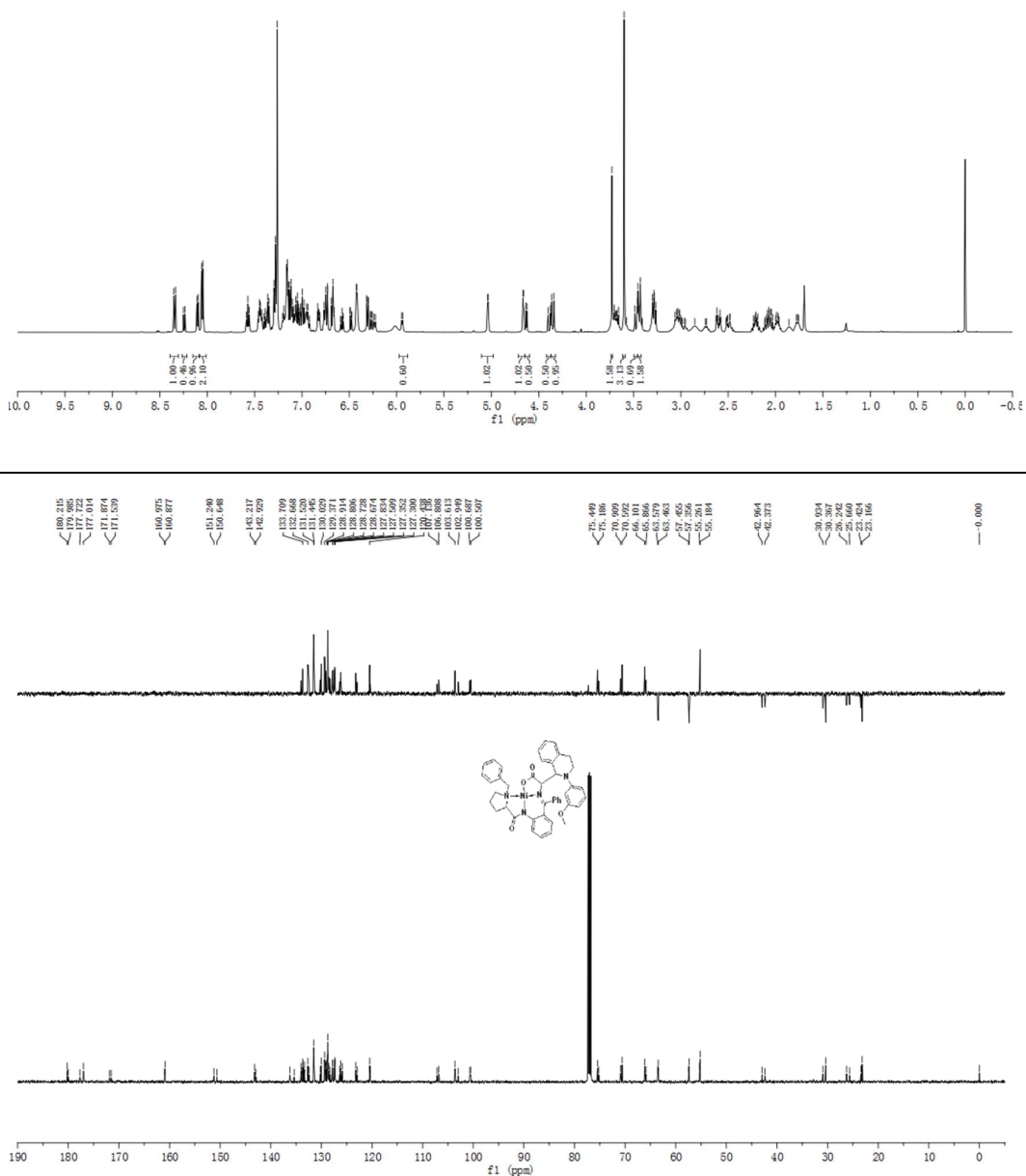
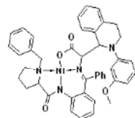
Schiff Base Complex 3a



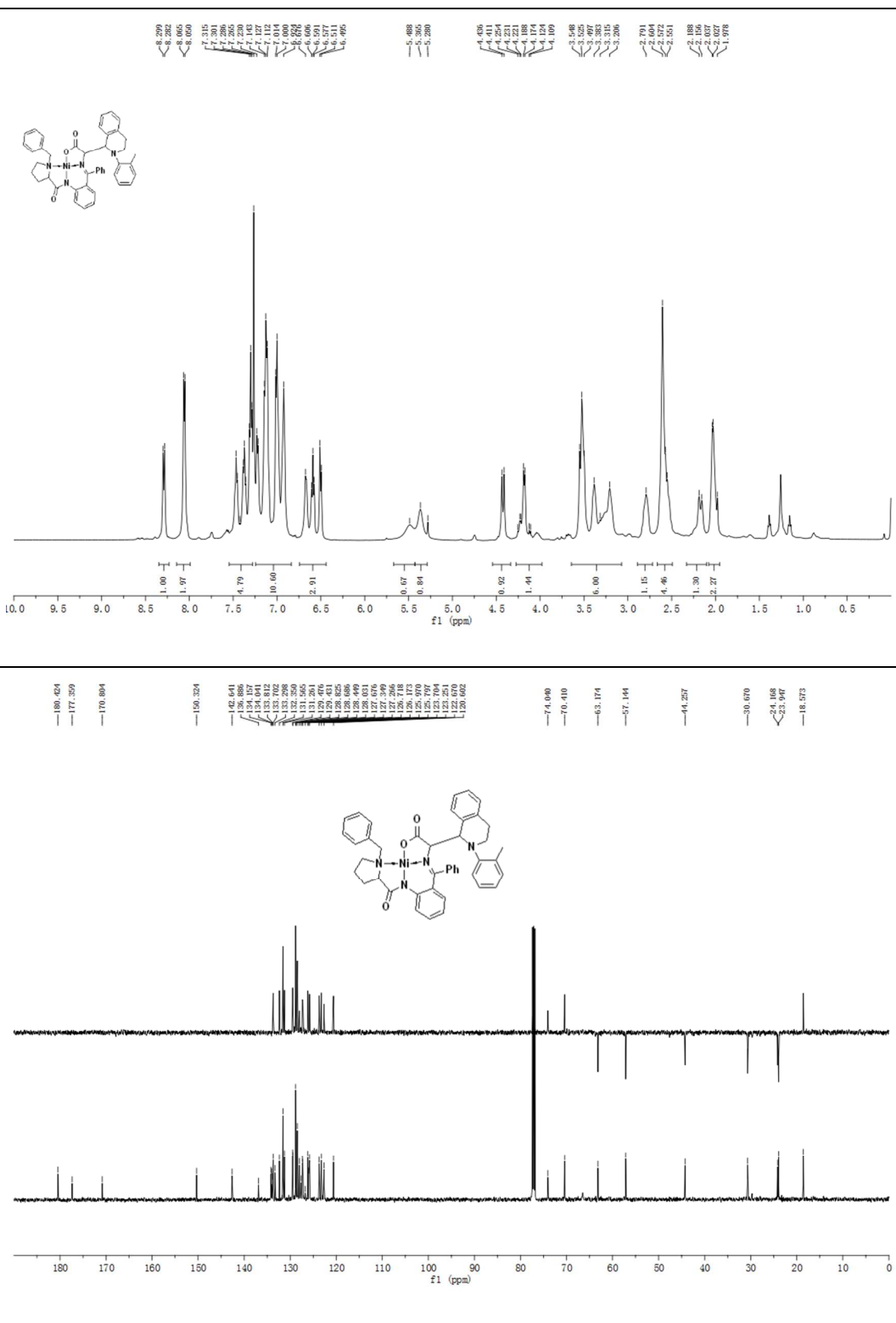
**Nickel(II)-(S)-BPB/2-amino-2-(4-methoxyphenyl)-1,2,3,4-tetrahydroisoquinolin-1-yl) acetic acid Schiff Base Complex 3b**



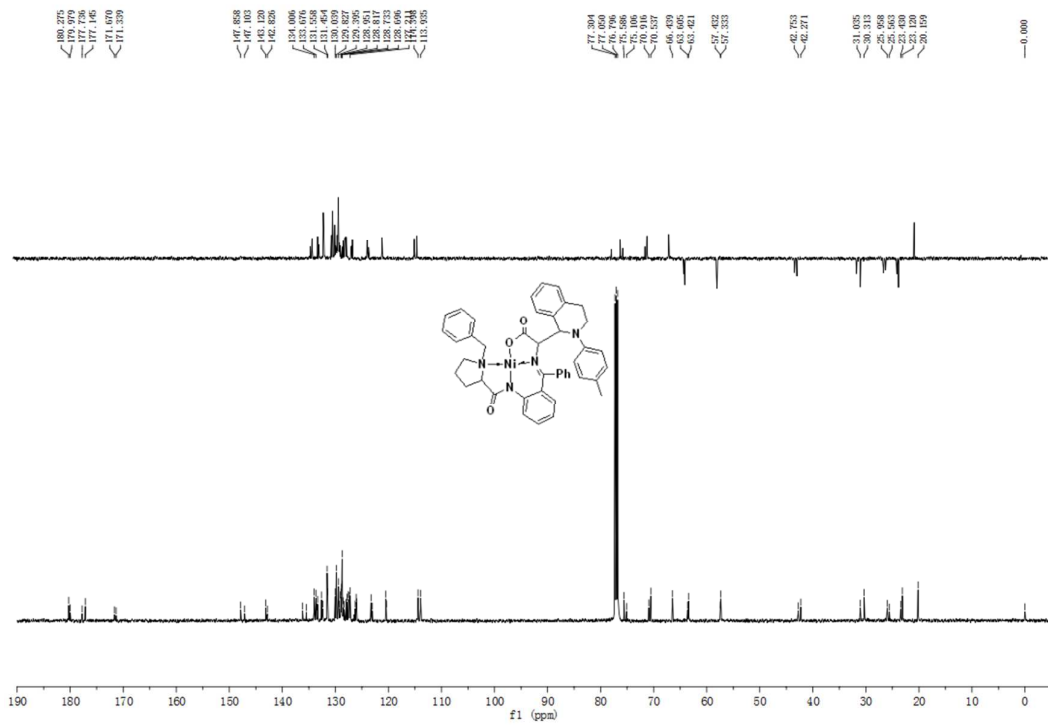
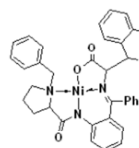
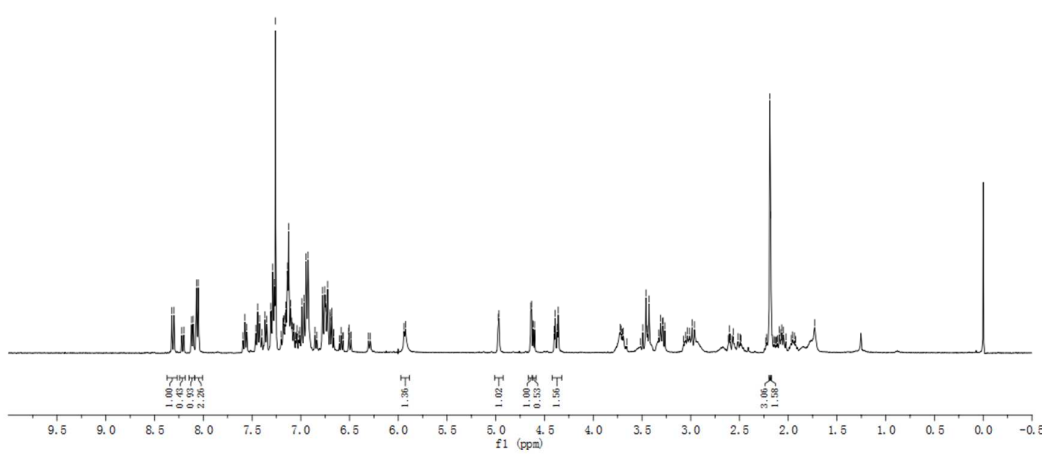
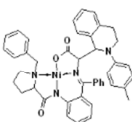
## Nickel(II)-(S)-BPB/2-amino-2-(2-(3-methoxyphenyl)-1,2,3,4-tetrahydroisoquinolin-1-yl)acetic acid Schiff Base Complex 3c



**Nickel(II)-(S)-BPB/2-Amino-2-(2-methylphenyl)-1,2,3,4-tetrahydroisoquinolin-1-yl) acetic acid Schiff Base Complex 3e**

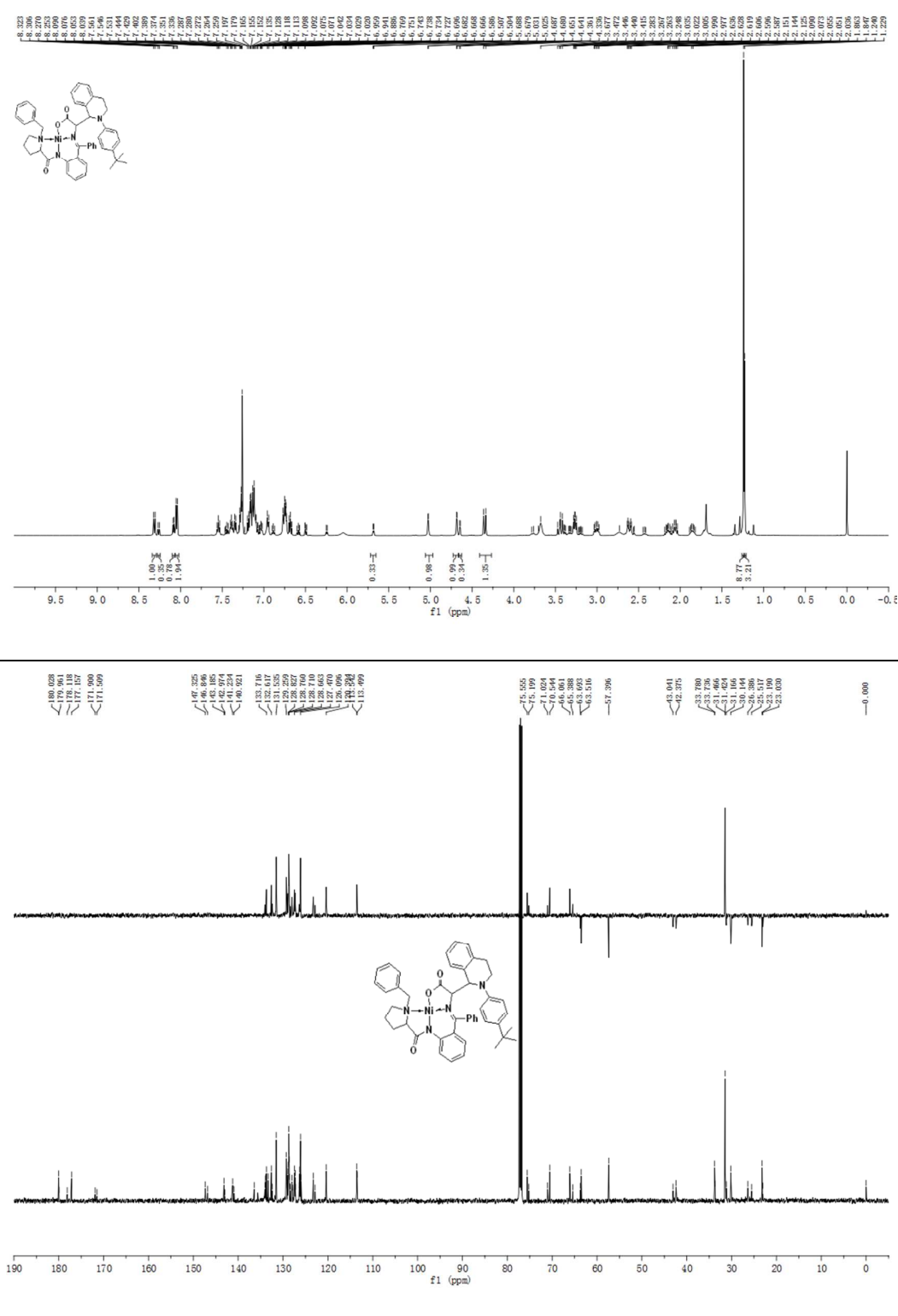


## Nickel(II)-(S)-BPB/2-Amino-2-(2-(4-methylphenyl)-1,2,3,4-tetrahydroisoquinolin-1-yl) acetic acid Schiff Base Complex 3f

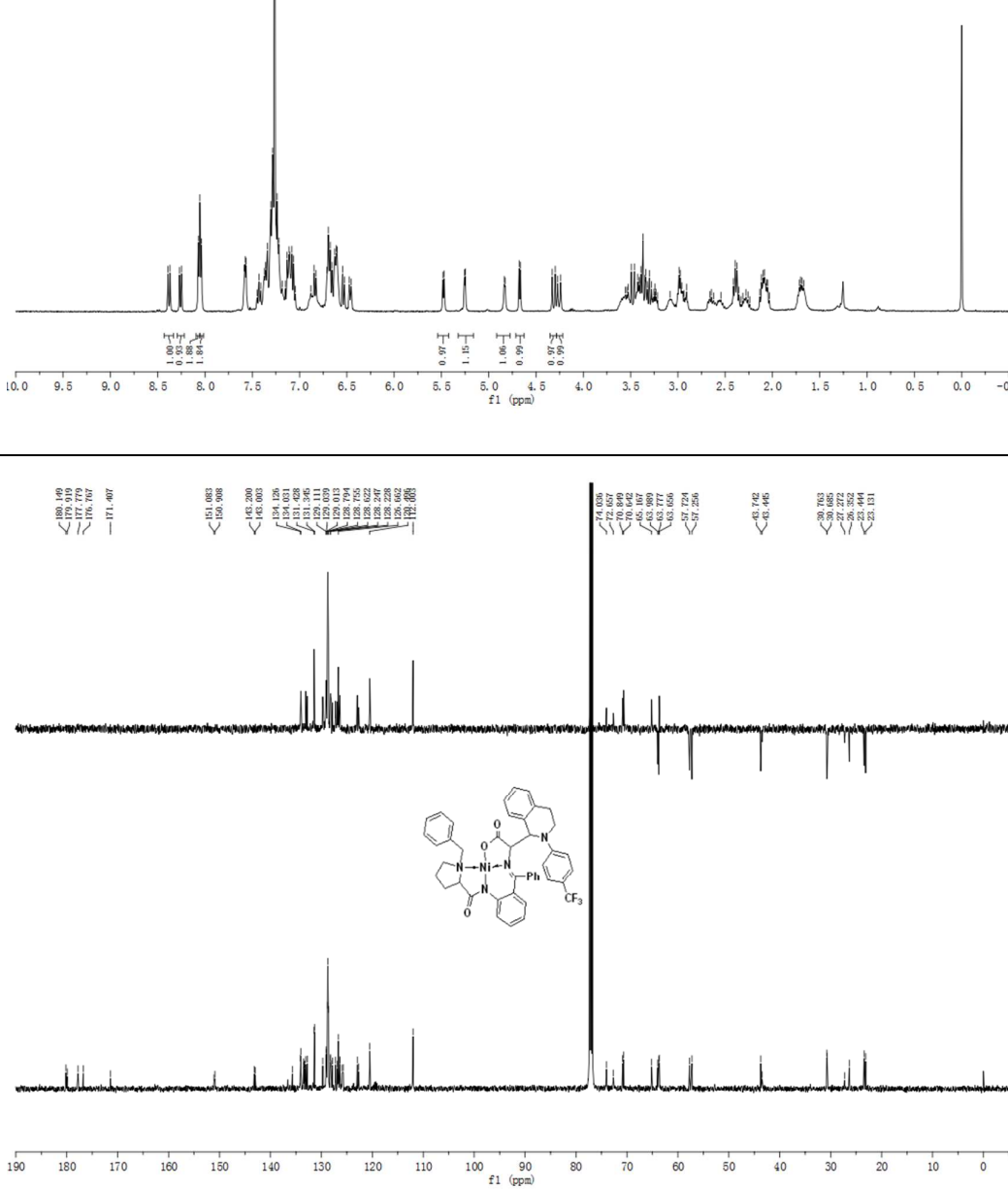


**Nickel(II)-(S)-BPB/2-Amino-2-(2-(4-tert-butylphenyl)-1,2,3,4-tetrahydroisoquinolin-1-yl)**

**acetic acid Schiff Base Complex 3g**



**Nickel(II)-(S)-BPB/2-Amino-2-(2-(4-(trifluoromethyl)phenyl)-1,2,3,4-tetrahydroisoquinolin-1-yl) acetic acid Schiff Base Complex 3h**



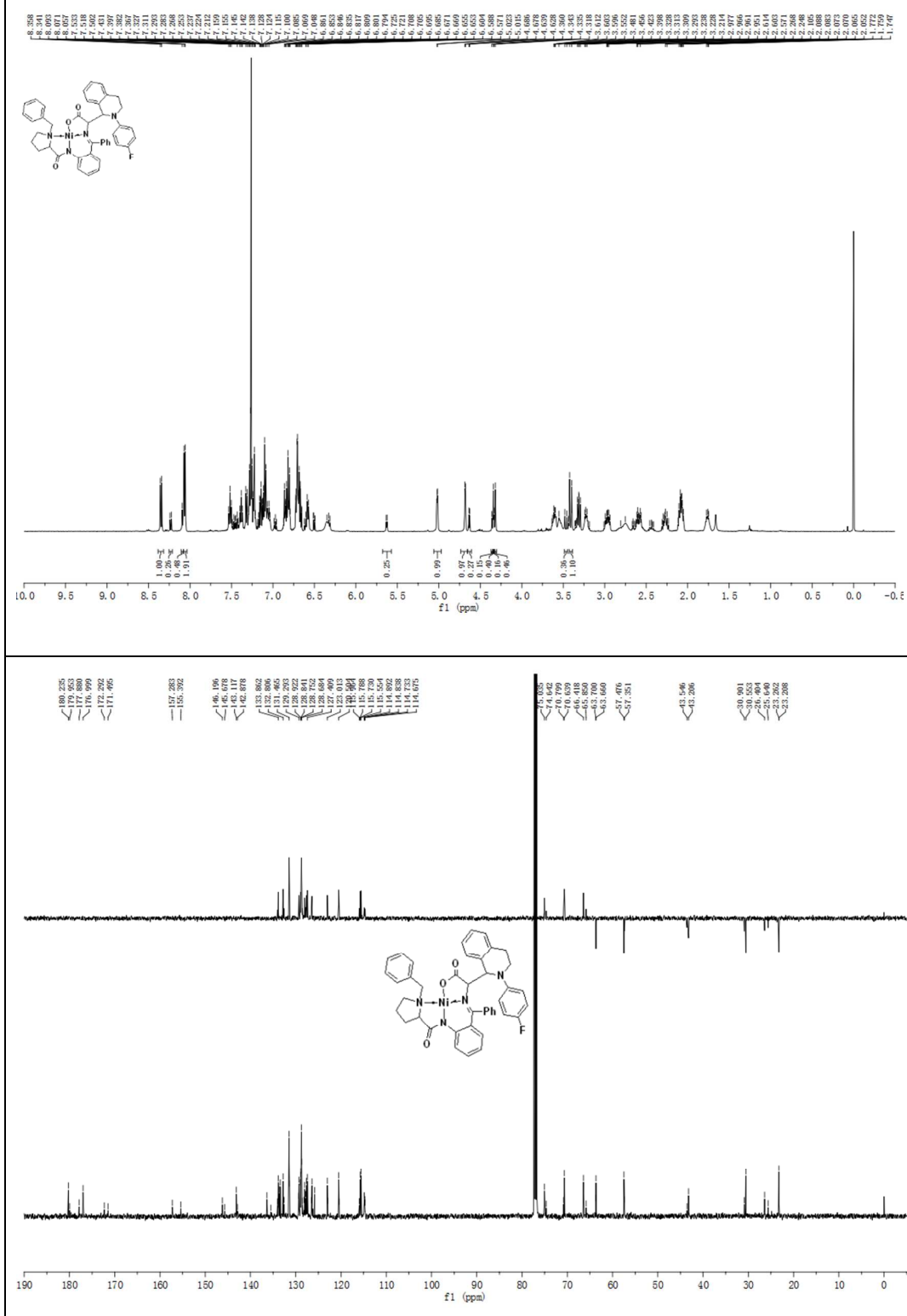
190 180 170 160 150 140 130 120 110 100 90 80 70 60 50 40 30 20 10 0

f1 (ppm)

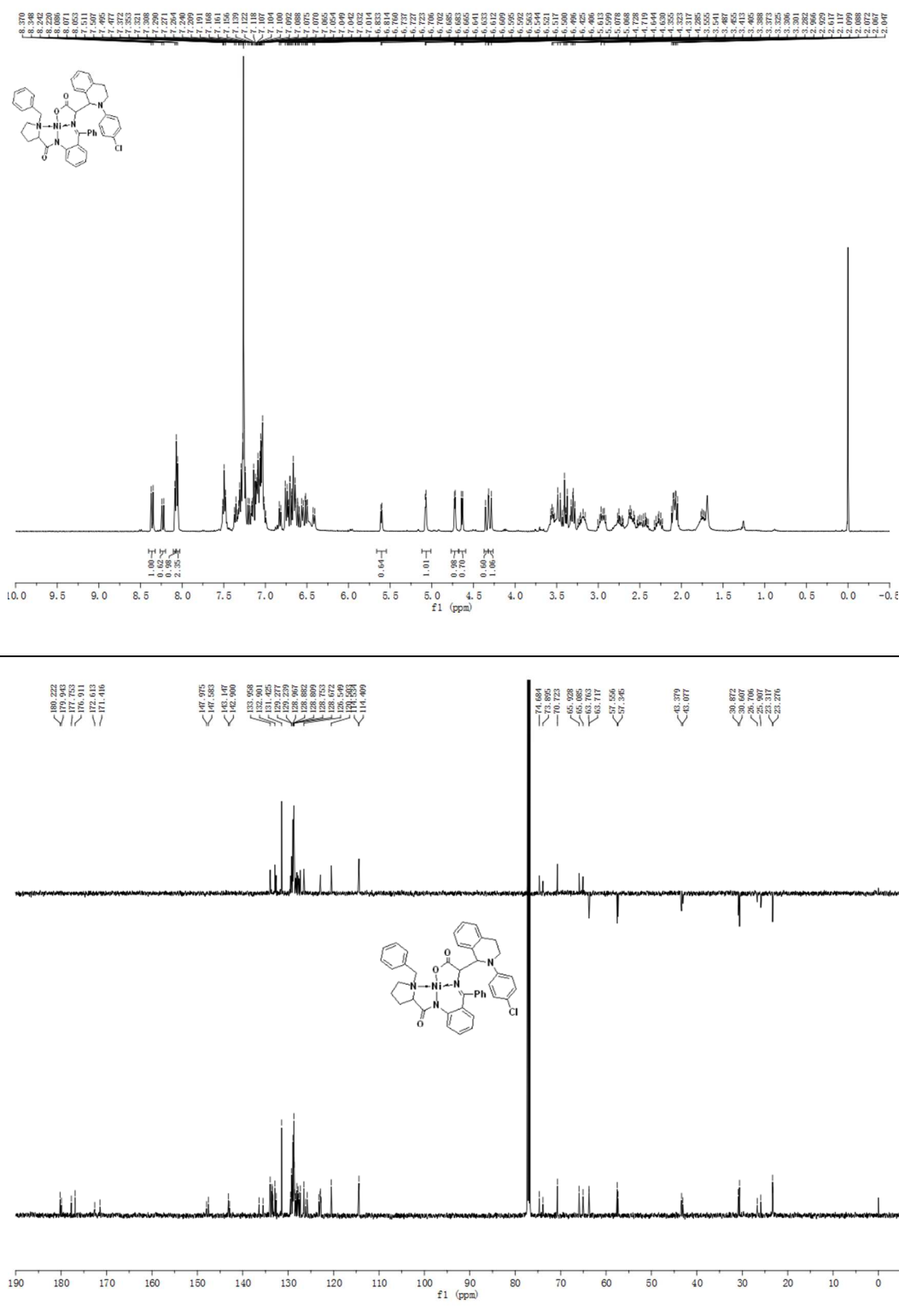
190 180 170 160 150 140 130 120 110 100 90 80 70 60 50 40 30 20 10 0

f1 (ppm)

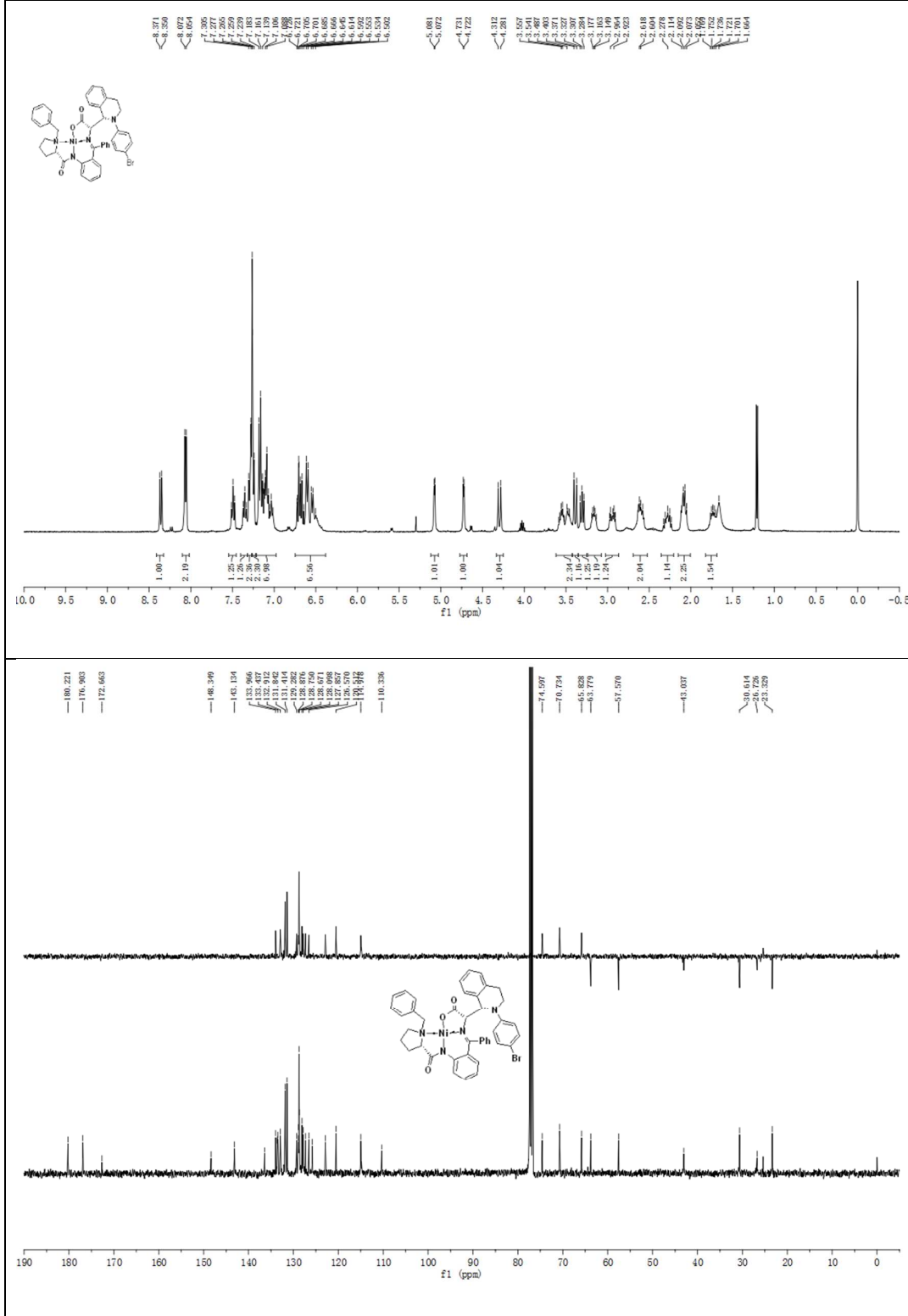
### Nickel(II)-(S)-BPB/2-Amino-2-(2-(4-fluorophenyl)-1,2,3,4-tetrahydroisoquinolin-1-yl) acetic acid Schiff Base Complex 3i



**Nickel(II)-(S)-BPB/2-Amino-2-(2-(4-chlorophenyl)-1,2,3,4-tetrahydroisoquinolin-1-yl) acetic acid Schiff Base Complex 3j**

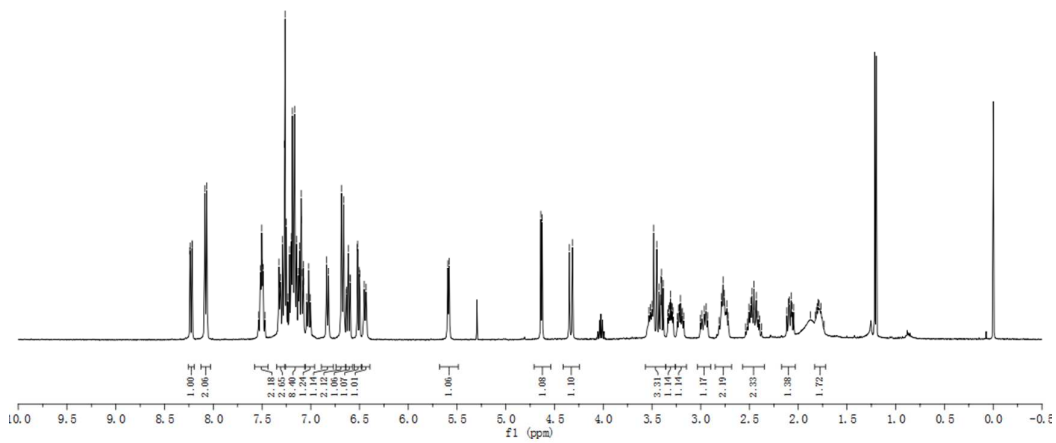
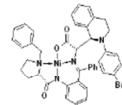


**Nickel(II)-(S)-BPB/(S)2-Amino-2-((S)-2-(4-bromophenyl))-1,2,3,4-tetrahydroisoquinolin-1-yl  
) acetic acid Schiff Base Complex 3k-syn**

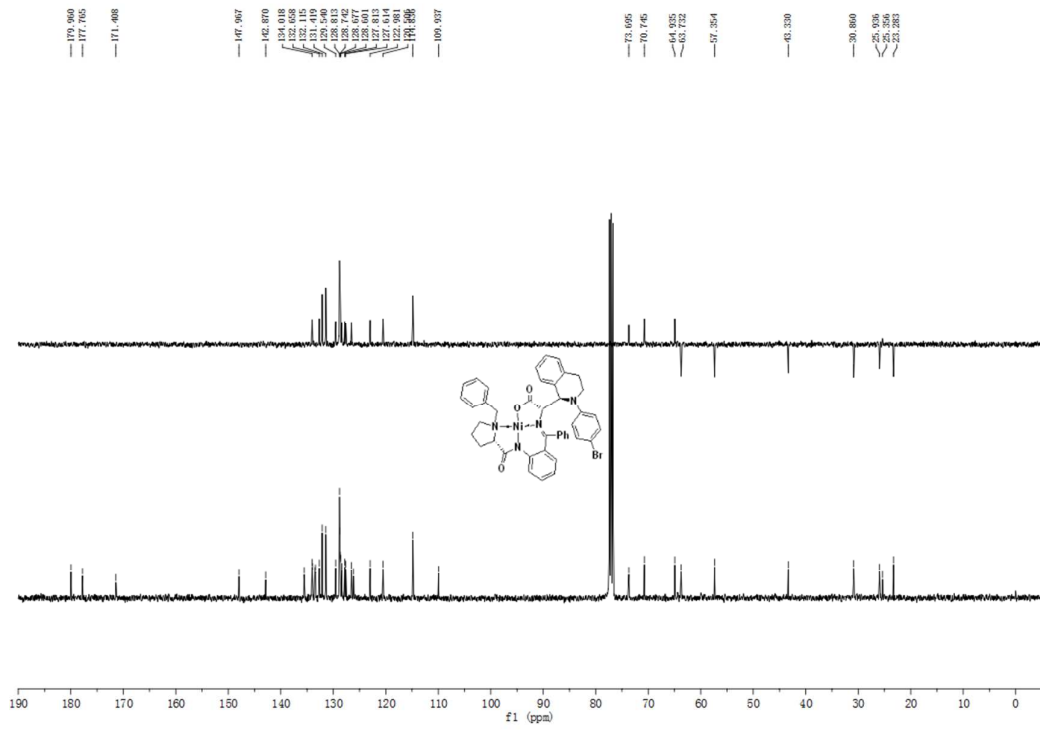


### Nickel(II)-(S)-BPB/(S)2-Amino-2-((R)-2-(4-bromophenyl))-1,2,3,4-tetrahydroisoquinolin-1-yl

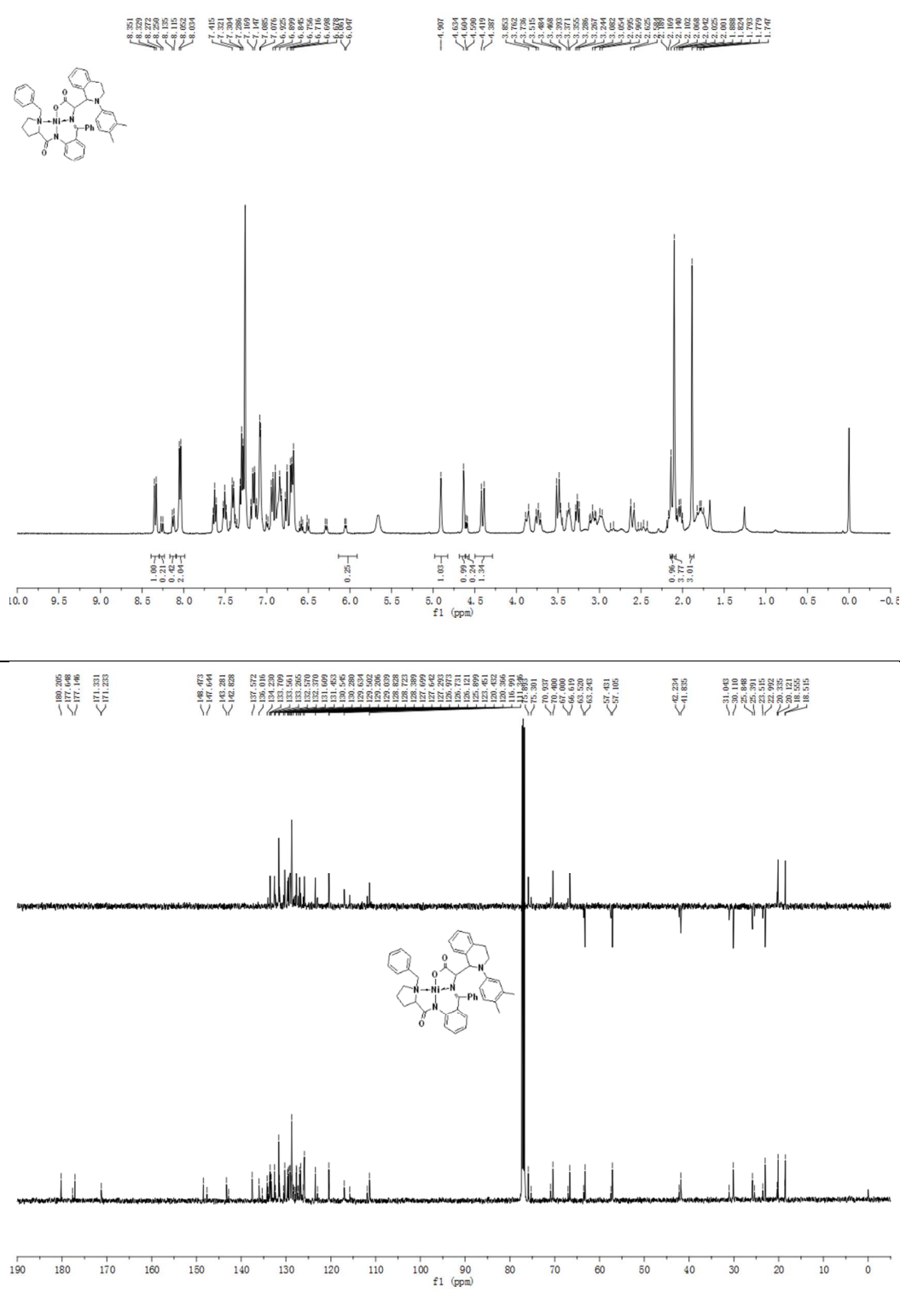
### ) acetic acid Schiff Base Complex 3k-*anti*



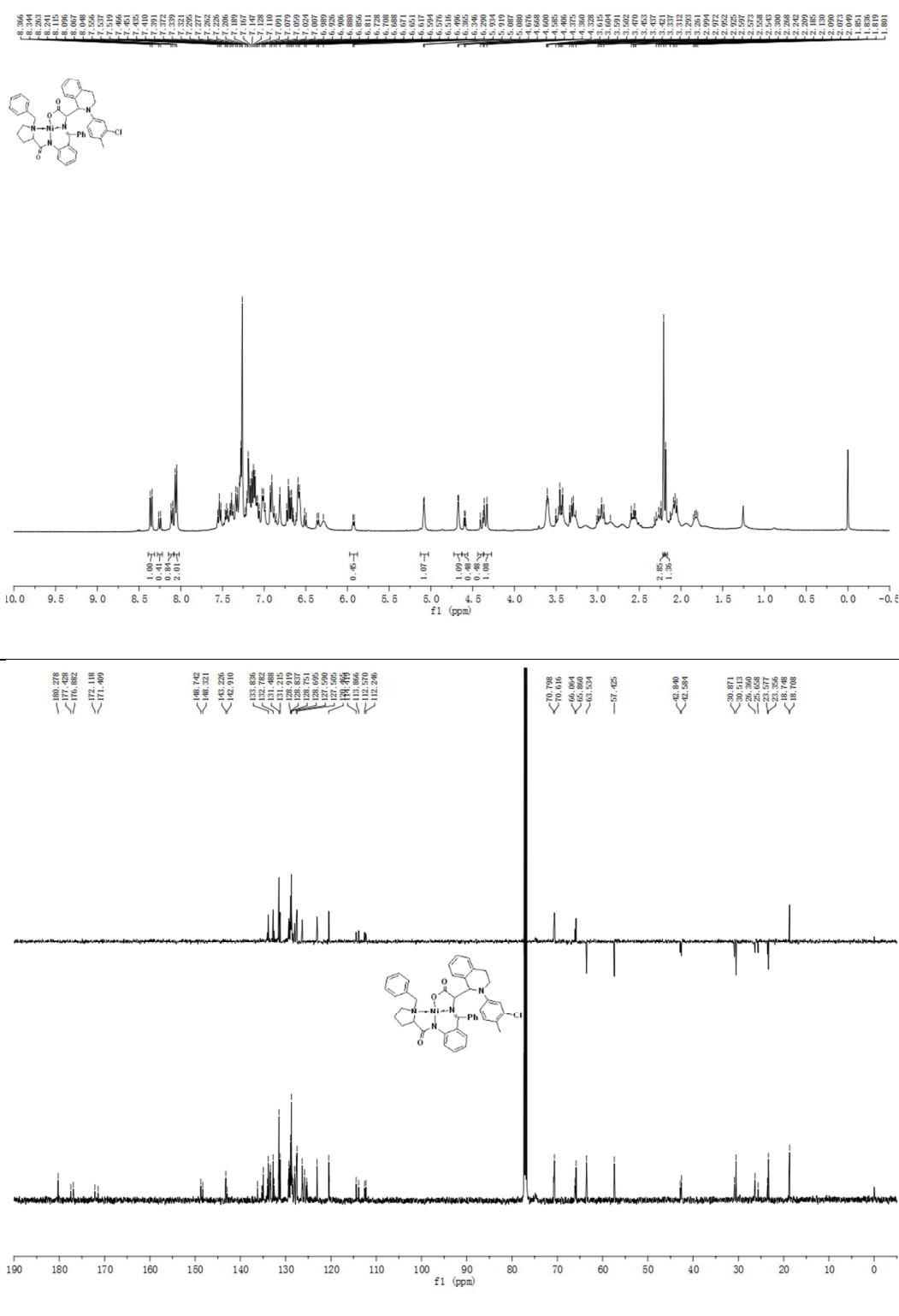
**— 179,960  
— 177,765  
— 171,408**



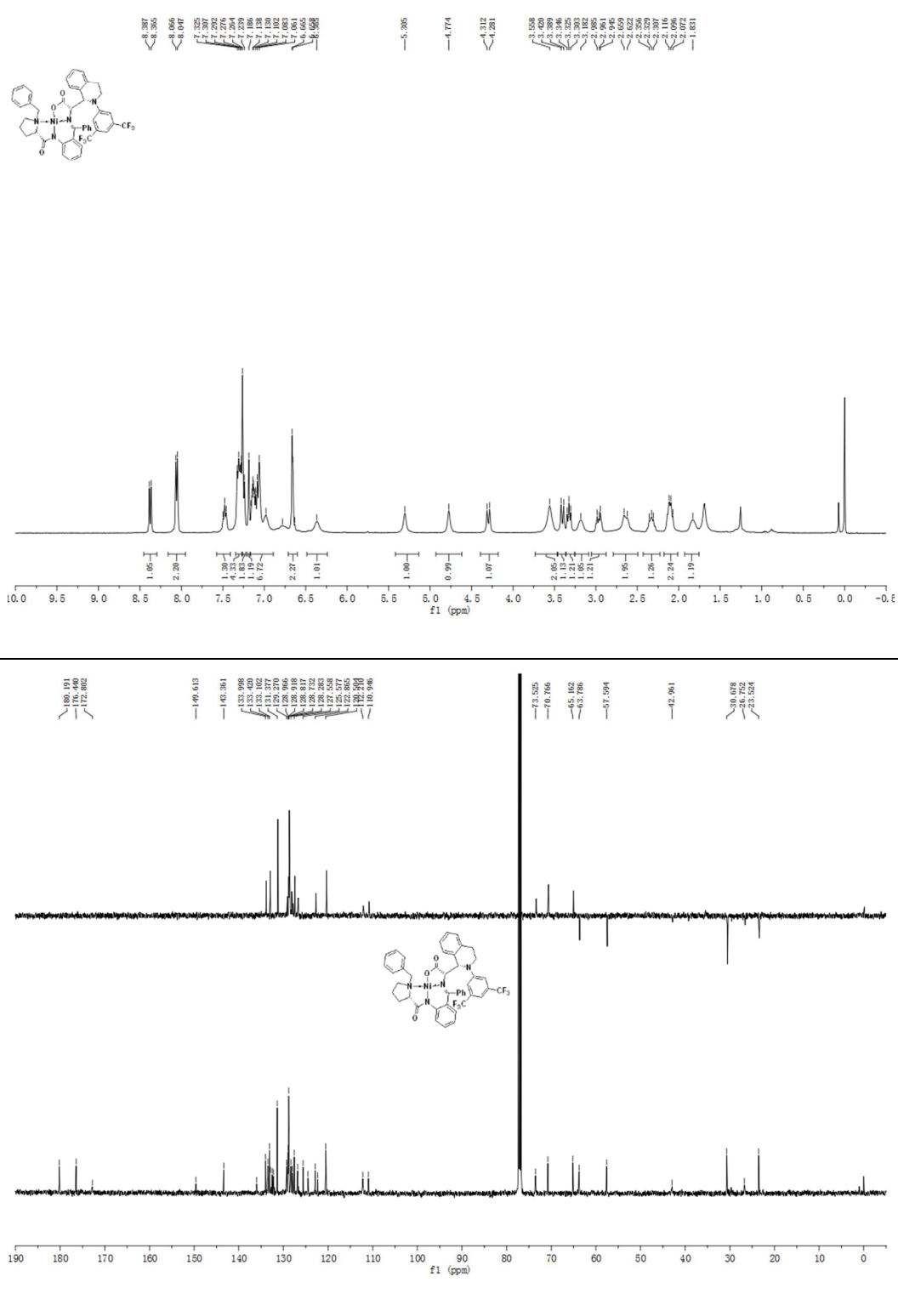
### Nickel(II)-(S)-BPB/2-Amino-2-(2-(3,4-dimethylphenyl))-1,2,3,4-tetrahydroisoquinolin-1-yl)acetic acid Schiff Base Complex 3l



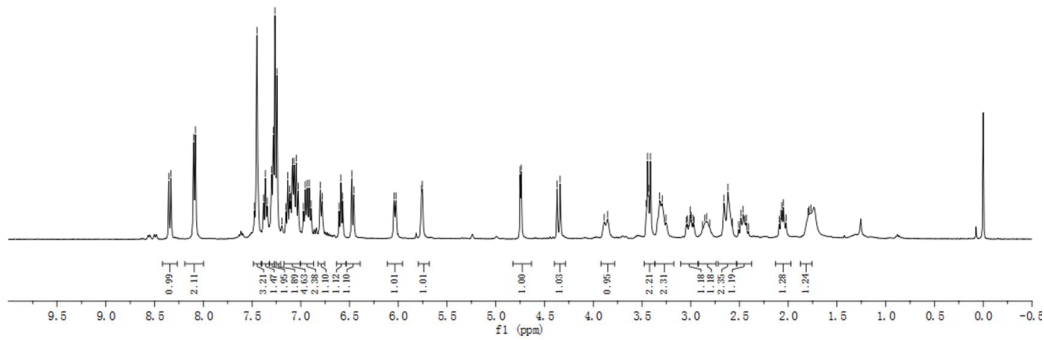
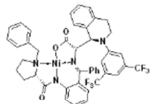
**Nickel(II)-(S)-BPB/2-Amino-2-(2-(3-chloro-4-methylphenyl))-1,2,3,4-tetrahydroisoquinolin-1-yl) acetic acid Schiff Base Complex 3m**



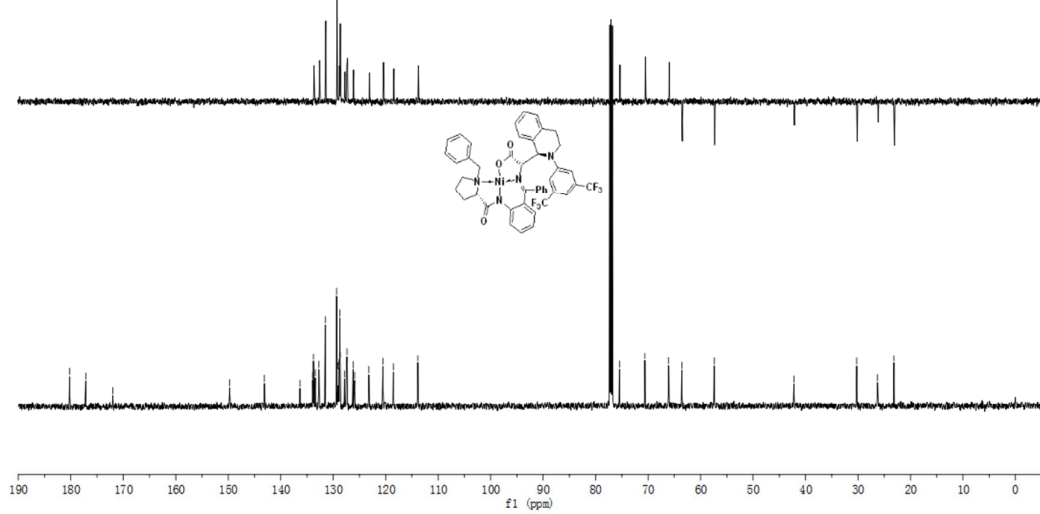
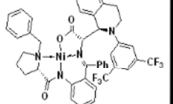
**Nickel(II)-(S)-BPB/(S)-2-Amino-2-((S)-2-(3,5-bis(trifluoromethyl)phenyl)-1,2,3,4-tetrahydroisoquinolin-1-yl) acetic acid Schiff Base Complex 3n-syn**



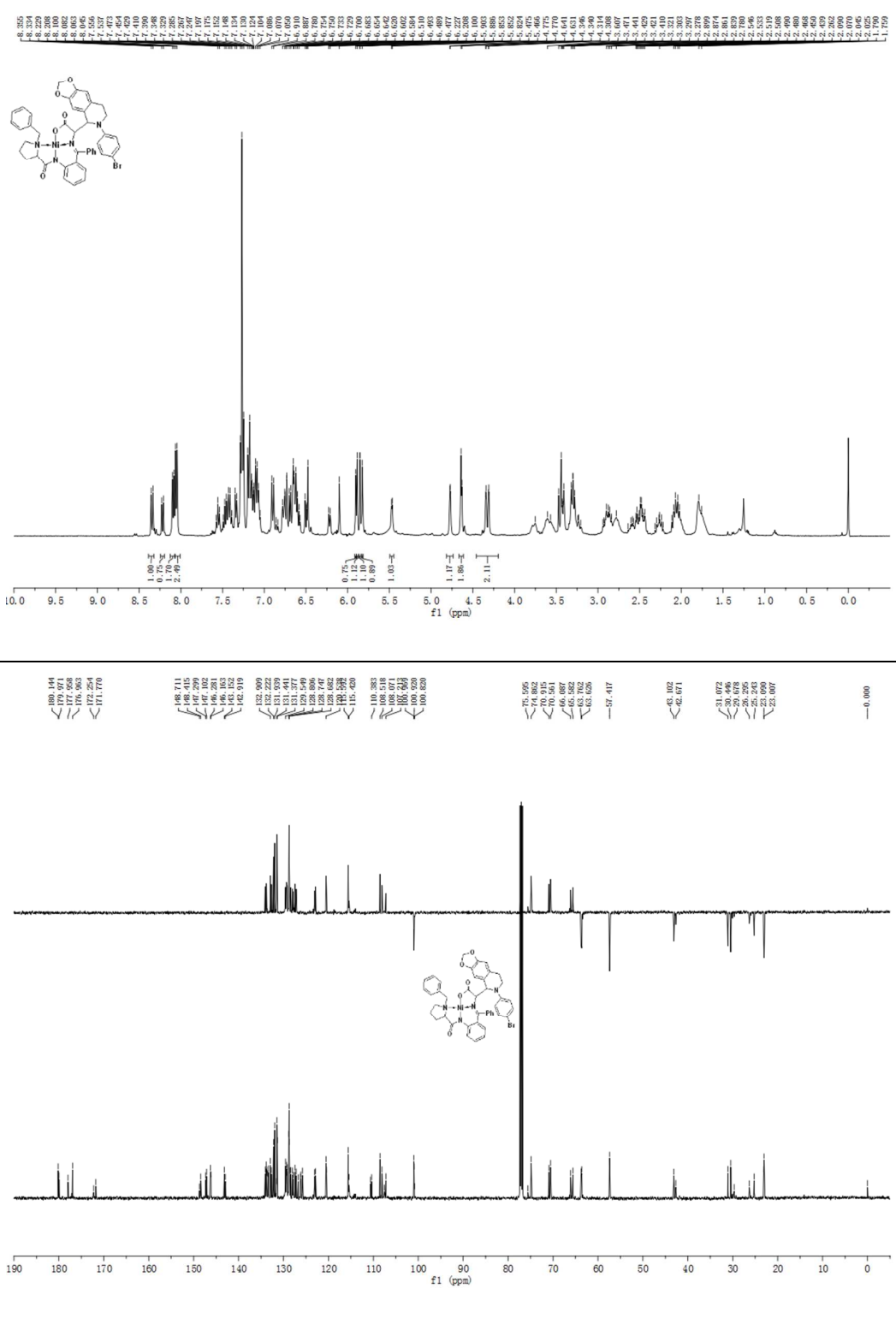
Nickel(II)-(S)-BPB/(S)-2-Amino-2-((R)-2-(3,5-bis(trifluoromethyl)phenyl)-1,2,3,4-tetrahydroisoquinolin-1-yl) acetic acid Schiff Base Complex 3n-*anti*



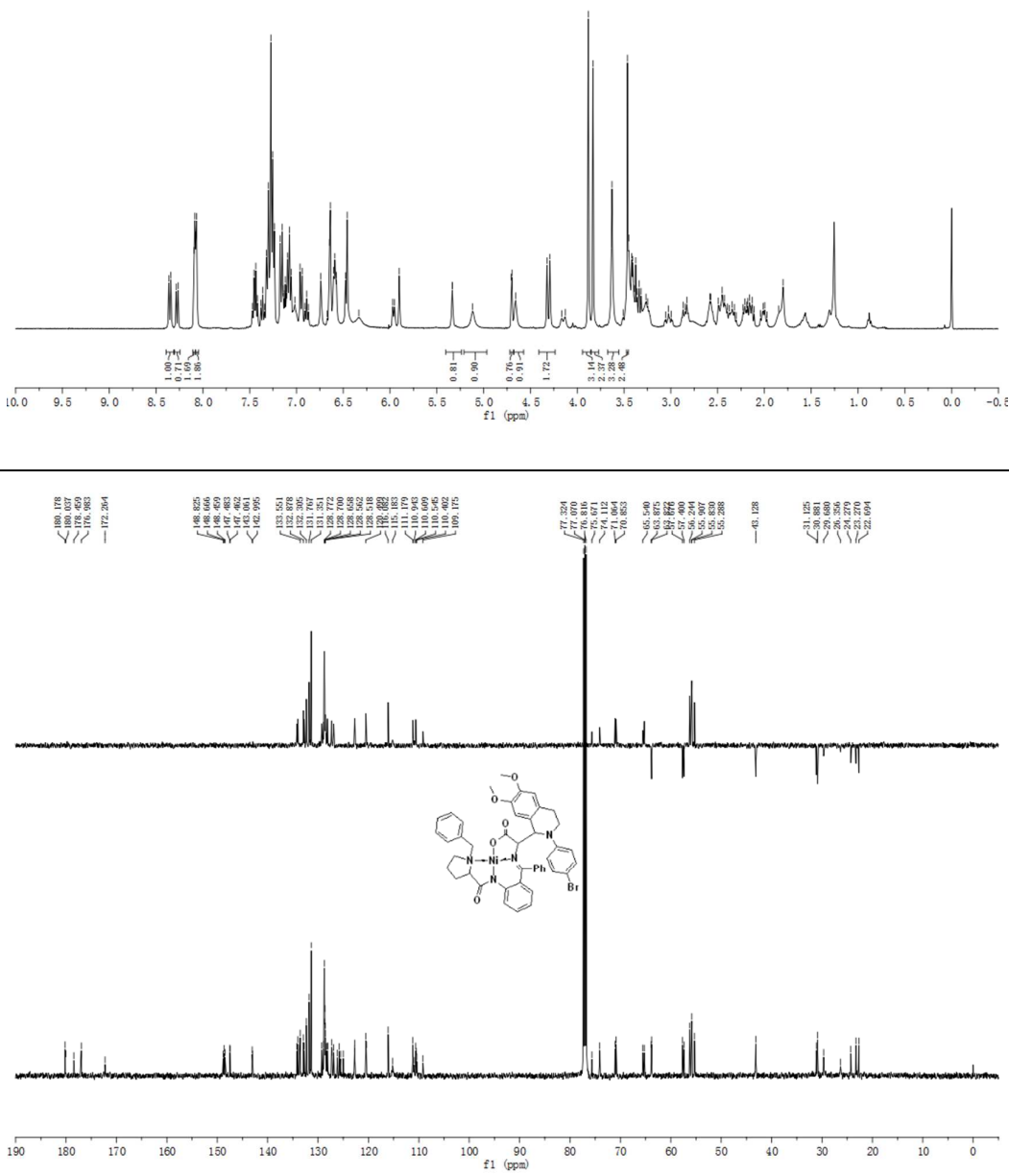
— 180, 207



**Nickel(II)-(S)-BPB/2-amino-2-((6-(4-bromophenyl)-5,6,7,8-tetrahydro-[1,3]dioxolo[4,5-g]isoquinolin-5-yl) acetic acid Schiff Base Complex 3o**

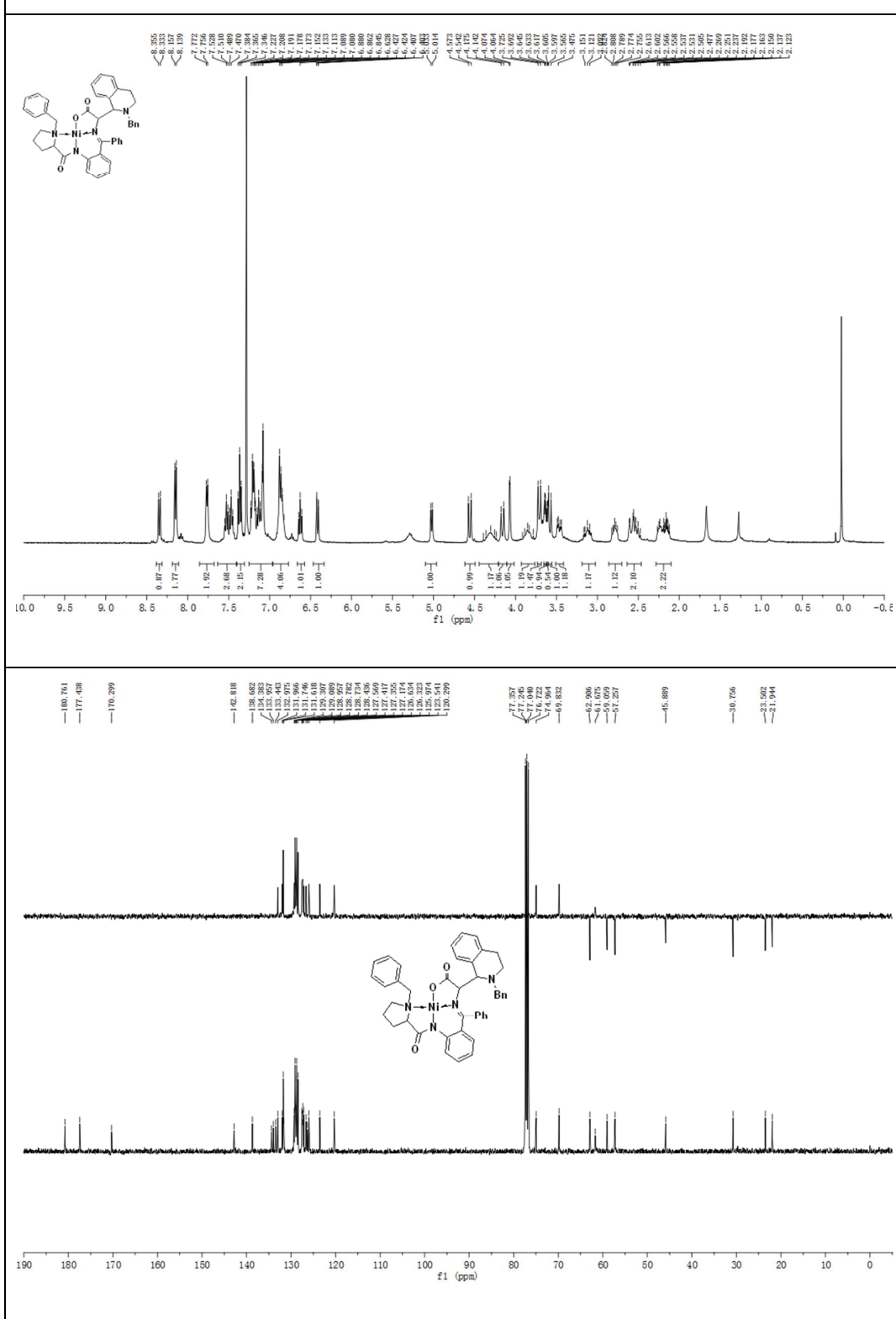


Nickel(II)-(S)-BPB/2-amino-2-(2-(4-bromophenyl)-6,7-dimethoxy-1,2,3,4-tetrahydroisoquinolin-1-yl) acetic acid Schiff Base Complex 3p

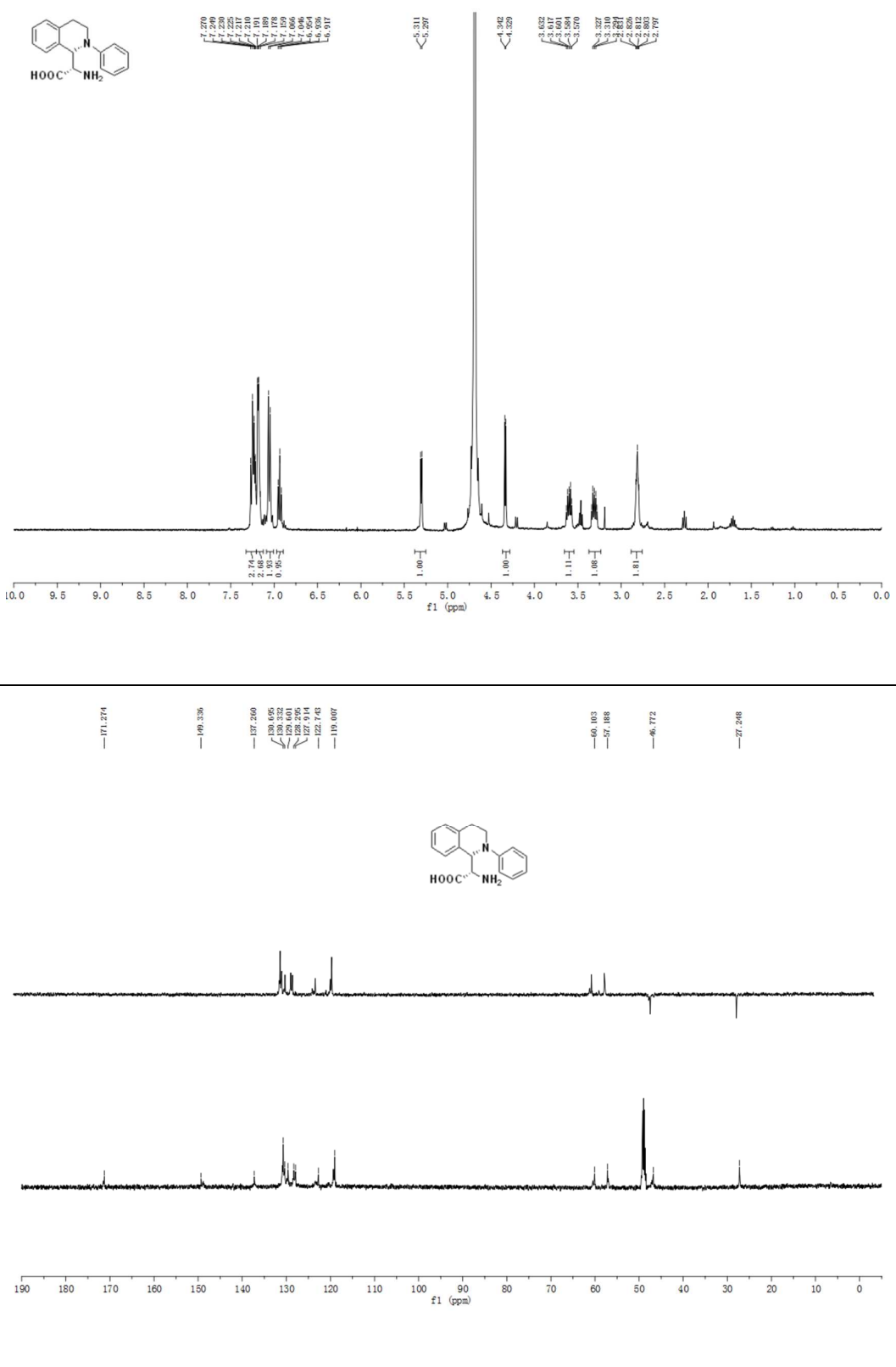


Nickel(II)-(S)-BPB/2-amino-2-(2-benzyl-1,2,3,4-tetrahydroisoquinolin-1-yl) acetic acid Schiff

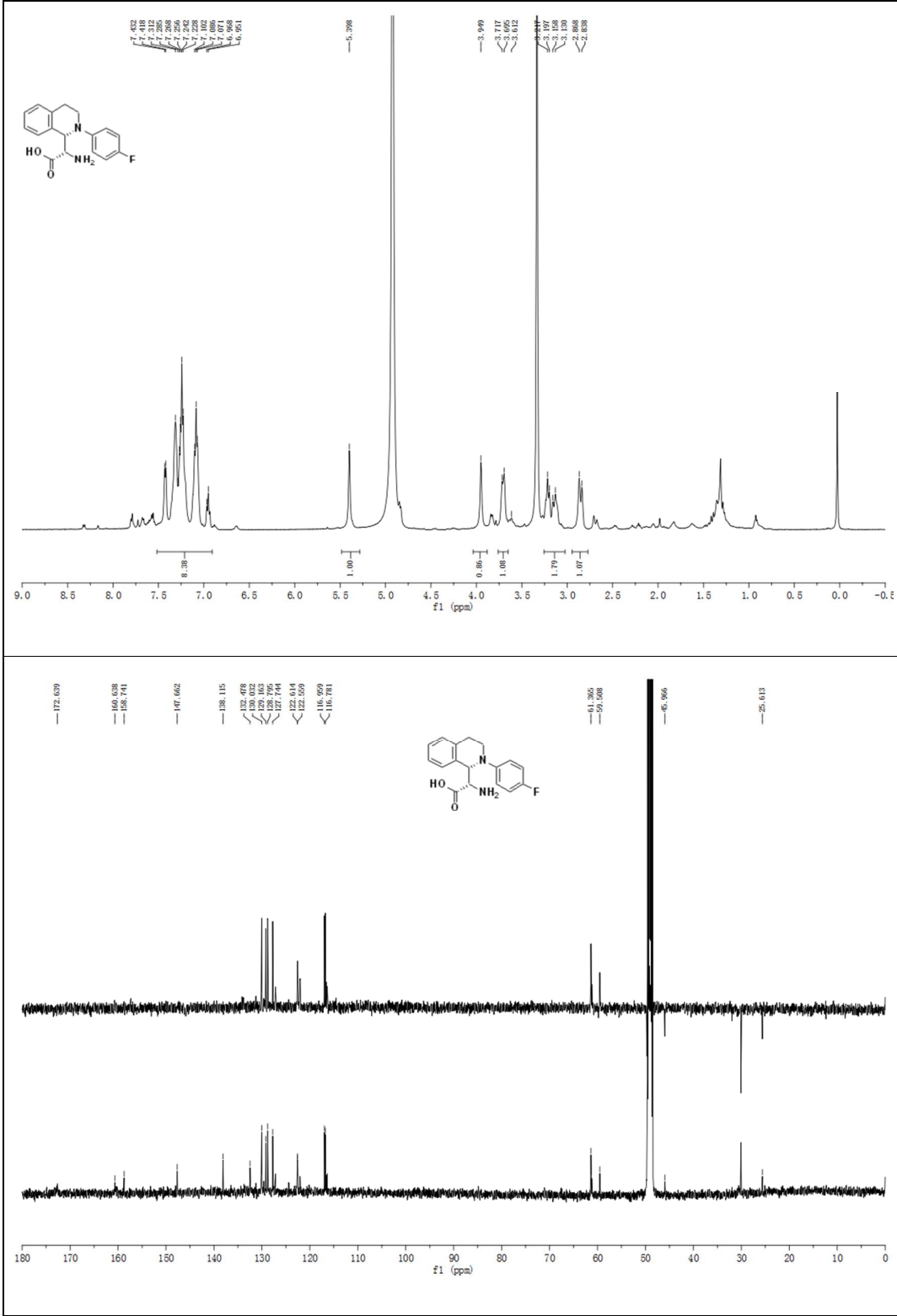
Base Complex 3q



**(S)-2-amino-2-((S)-2-phenyl-1,2,3,4-tetrahydroisoquinolin-1-yl)acetic acid 4a**



**(S)-2-amino-2-((S)-2-(4-fluorophenyl)-1,2,3,4-tetrahydroisoquinolin-1-yl)acetic acid 4i**



## (G) References

- (1) For recent reviews on CDC, see: (a) Li, C. J.; Li, Z. P. *Pure Appl. Chem.* **2006**, *78*, 935-945.  
(b) Li, C. J. *Acc. Chem. Res.* **2009**, *42*, 335-344. (c) Scheuermann, C. J. *Chem. Asian J.* **2010**, *5*, 436-451. (d) Cho, S. H.; Kim, J. Y.; Kwak, J.; Chang, S. *Chem. Soc. Rev.* **2011**, *40*, 5068-5083. (e) Wendlandt, A. E.; Suess, A. M.; Stahl, S. S. *Angew. Chem. Int. Ed.* **2011**, *50*, 11062-11087. (f) Yeung, C. S.; Dong, V. M. *Chem. Rev.* **2011**, *111*, 1215-1292.
- (2) Zhang, G.; Zhang, Y.; Wang, R. *Angew. Chem. Int. Ed.* **2011**, *50*, 10429-10432.
- (3) Zhang, J.; Tiwari, B.; Xing, C.; Chen, X.; Chi, Y. R. *Angew. Chem. Int. Ed.* **2012**, *51*, 3649-3652.
- (4) Soloshonok, V. A.; Avilov, D. V.; Kukhar, V. P.; VanMeervelt, L.; Mischenko, N. *Tetrahedron Lett.* **1997**, *38*, 4671-4674.
- (5) Wang, J.; Shi, T.; Deng, G. H.; Jiang, H. L.; Liu, H. *J. Org. Chem.* **2008**, *73*, 8563-8570.
- (6) Lin, D. Z.; Wang, J.; Zhang, X.; Zhou, S. B.; Lian, J.; Jiang, H. L.; Liu, H. *Chem. Commun.* **2013**, *49*, 2575-2577.